IDENTIFYING SEASONAL CHANGES IN STREAMBED THERMAL PROFILE

IN A THIRD ORDER AGRICULTURAL STREAM

USING 2D THERMAL MODELING

Hridaya Bastola

56 Pages December 2010

This study identifies the seasonal changes in the streambed temperature profile of a low gradient agricultural stream and finds how hydraulic and thermal properties of the streambed change.

APPROVED:

_____

Date Eric W. Peterson, Chair

_____

Date Stephen J. Van der Hoven

_____

Date Dagmar Budikova

IDENTIFYING SEASONAL CHANGES IN STREAMBED THERMAL PROFILE IN A THIRD ORDER AGRICULTURAL STREAM USING 2D THERMAL MODELING

Hridaya Bastola

56 Pages December 2010

The thermal profile of a streambed is affected by a number of factors including temperature of both stream water and ground water, hydraulic conductivity, thermal conductivity and heat capacity of the streambed, and the nature of hyporheic flowpaths. Changes in these parameters over time, thus, cause changes in thermal profiles. In the study, temperature data were collected at depths of 30, 60, 90 and 150 cm at six hyporheic wells 5 meters apart along the thalweg of a third-order, low gradient stream. A positive temperature gradient with inflection at 90 cm depth was observed during the summer period while a negative temperature gradient with inflection at 30 cm was observed during the winter period suggesting greater influence of stream water temperatures in the substrate during the summer. Bromide tracer test done in the study area suggested a shallow local hyporheic extent that was mostly consistent with the upwelling conditions suggested by the model. Thermal models of the streambed were built using VS2DHI to simulate the thermal profiles observed in the field. During the calibration of the models, deviations from observed temperature were calculated using mean absolute error (MAE). Sensitivities of hydraulic and thermal parameters used in the

model were identified and the more sensitive parameters were first corrected before adjusting for the less sensitive parameters. The spring model improved to a MAE of 0.2°C after adjusting parameter values. The spring model was not the best fit model when used for week long periods in summer and winter yielding MAE of 1.0°C and 0.9°C respectively. Adjustments to the parameters resulted in MAE of 0.4°C and 0.3 °C for respective models. Comparison of the parameters along with analysis of temperature envelopes and Peclet numbers suggested greater upwelling, and stability in temperatures, during the winter than during the summer. Upwelling was more pronounced in the upstream reach of the pool in the riffle and pool sequence and underlines its importance to benthic organisms as a favorable refuge from the winter cold and possibly from summer heat.

APPROVED:

_____

Date Eric W. Peterson, Chair

_____

Date Stephen J. Van der Hoven

_____

Date Dagmar Budikova

IDENTIFYING SEASONAL CHANGES IN STREAMBED THERMAL PROFILE IN A THIRD ORDER AGRICULTURAL STREAM USING 2D THERMAL MODELING

HRIDAYA BASTOLA

A Thesis Submitted in Partial
Fulfillment of the Requirements
for the Degree of

MASTER OF SCIENCE

Department of Geography-Geology

ILLINOIS STATE UNIVERSITY

2010

IDENTIFYING SEASONAL CHANGES IN STREAMBED THERMAL PROFILE IN A THIRD ORDER AGRICULTURAL STREAM USING 2D THERMAL MODELING

HRIDAYA BASTOLA

THESIS APPROVED:

_____

Date Eric W. Peterson, Chair

_____

Date Stephen J. Van der Hoven

_____

Date Dagmar Budikova

ACKNOWLEDGEMENT

I would like to thank Dr. Eric W. Peterson, Dr. Stephen J. Van der Hoven and Dr. Dagmar Budikova for all the help and guidance during the course of the study. Dr. Eric W. Peterson's input and knowledge on the subject was paramount in the evolution of the study and in bringing the thesis to its present form. Insightful suggestions and comments from Dr. Stephen J. Van der Hoven were very helpful in improving my thesis. I would also like to thank Illinois Groundwater Association for funding part of the project. This work would have been far from possible without the help in field work from fellow graduate and undergraduate students especially Erasmus Oware. Finally, I am grateful for all the support from my family.

I dedicate this thesis to my mother.

H.B.

CONTENT

ACKNOWLEDGEMENT i

CONTENTS II

TABLES III

FIGURES IV

CHAPTER

I. INTRODUCTION 1

Hyporheic Zone 3
Significance 4
Statement of the Problem 5
Study Area 5
Climate and Precipitation 8

II. METHOD 10

Hyporheic Wells and Piezometers 10
Data Collection 11
Scour and Fill 13
Tracer Test 13
Thermal Modeling 14

III. RESULTS 18

Streambed Topography 22
Tracer Test 23
Temperature Models 24
Parameter Values and Sensitivity Analysis 33

IV. DISCUSSION 36

V. CONCLUSION 44

REFERENCES 46

APPENDIX A: Scour and Fill and Elevation Data 50

APPENDIX B: Tracer Test Data 51

APPENDIX C: Matlab Program to Get Error Output File 53

APPENDIX D: Matlab Program to Calculate MAE 56

TABLES

Table Page

1. Representative value ranges for hydraulic and thermal parameters. 16
2. Temperature ranges and averages for the three model periods. 19
3. Parameter values for the best fit models for the spring, summer and winter time periods. 33
4. Table of Peclet no. for various wells during the three model periods. 43

FIGURES

Figure		Page
1.	Types of hyporheic flows. A-A' shows transverse hyporheic flow and B-B' shows various extents of longitudinal hyporheic flows.	4
2.	Location of the study site in the Little Kickapoo Creek, Heyworth, IL.	6
3.	Schematic cross-section for AA’ showing the three geologic units.	7
4.	Schematic setup of hyporheic wells (1-6) and stilling well (S) in the study site.	12
5.	Design of individual hyporheic wells.	12
6.	Conceptual model of the streambed showing location of the temperature loggers.	15
7.	Graph showing stream stage, ground water and stream temperatures over the period of data collection.	19
8.	Stage, surface and subsurface temperatures during the spring model week.	20
9.	Stage, surface and subsurface temperatures during the summer model week.	21
10.	Stage, surface and subsurface temperatures during the spring model week.	22
11.	Streambed profile changes from February to October.	23
12.	Bromide concentrations for sample points with higher concentrations of bromide.	24
13.	Best fit VS2DH models simulating streambed temperature distribution for the spring model period.	26
14.	Best fit VS2DH models simulating streambed temperature distribution for the summer model period.	27
15.	Best fit VS2DH models simulating streambed temperature distribution for the winter model period.	28
16.	Error graphs for the spring time period at depths of a) 30 cm, b) 60 cm, c) 90 cm and d) 150 cm.	29
17.	Error graphs for the summer time period at depths of a) 30 cm, b) 60 cm, c) 90 cm and d) 150 cm.	30

18. Error graphs for the winter time period at depths of a) 30 cm, b) 60 cm, c) 90 cm and d) 150 cm. 31

19. Comparison of observed and simulated temperature for Well 3 for spring, summer and winter model periods a)-c) respectively. 32

20. Model sensitivity analysis for a) Spring, b) Winter and c) Summer models. 35

21. Temperature envelopes for Well 1-6. 38

CHAPTER I

INTRODUCTION

Heat transmitted to the Earth's surface is predominantly from the sun; only a tiny fraction- about 1/5000th of the total energy transmitted to the Earth's surface is from the heated internal core (Bukata et al, 1995). With almost no radiation being received from the sun and due to radiant heat loss to the atmosphere during the night, surface temperatures at night tend to be cooler than during the day resulting in daily fluctuations in sediment surface temperatures. Also, the distance of the Sun from the Earth and the tilt axis causes seasonal variations in surface temperatures. The fluctuation in surface temperatures was identified as the origin of thermal interaction between sediments at different depths on a streambed (Stallman, 1965). These fluctuations at the land surface cause propagation of heat energy through conduction and advection. The later of these phenomena imparts distinctive thermal patters to streams.

The use of streambed temperatures in studying ground water is a fairly recent development. One of the earliest studies was done by Stallman (1963) who realized the potential of using temperature measurements to solve the inverse problem for ground water velocity and hydraulic conductivity. After the interest revived in the late 1980's, one of the notable works using streambed temperatures was done in identifying gaining vs. losing portions of small creek in northern Indiana (Silliman and Booth, 1993). Time series measurements of sediment temperature and water temperature were compared to identify regions of ground water inflow and outflow relative to surface waters. Further work was later done to quantify the downflow through the stream (Silliman et al, 1995). In the model, the thermal and hydraulic properties were assumed to remain constant in time and space, the velocity of water in the sediment was assumed to be one dimensional in the vertical direction, and all other effects of chemical and biological processes in advection and conduction including hydrodynamic dispersion were assumed negligible. The model was used to estimate temperature patters for different flux ranges and later compared to the temperature patterns in a losing portion of the study stream.

Bravo and Jiang (2002) used HST3D, a three-dimensional, finite differences model to estimate hydraulic conductivity and inflow to a wetland system from head and temperature data. The model estimate for hydraulic conductivity range and flux closely represented the measurements in the fields. A similar study to estimate hydraulic conductivity in a stream was done using VS2DHI, a graphical software based on VS2DH (Su et al., 2004). The study used water levels and seasonal temperatures to estimate hydraulic conductivities in a stream-aquifer system in Sonoma County, California. Comparative study of the hydraulic gradient, hydraulic conductivity and percolation rate

has been successfully done using VS2DT, a solute transport model, and VS2DH using bromide and heat respectively (Constantz et al., 2003). The study concluded that the hydraulic parameters estimation using bromide and temperature are of comparable quantitative value and that heat being a non conservative tracer is a poor method to identify preferential flowpaths.

A method to quantify surface water –ground water interaction was developed using time series analysis of streambed thermal records from known depths (Hatch et al, 2006). With growing confidence in the methods developed, use of sediment thermal data to determine reasonable ground water flux rates is likely to be an effective field method that is quicker and more cost effective than setting up piezometers or seepage meters (Schmidt et al, 2007).

Hyporheic Zone

The region around a stream where surface water and ground water mixing occurs is referred to as the hyporheic zone. Depending on the field of interest, the hyporheic zone may be defined in light of nutrient transport (Triska et al., 1989), ecological processes (Boulton et al., 1998; Stanford and Ward, 1988) and on flow geometry (White, 1993, Winter et al., 1998). Nutrients, biota and physical characteristics like temperature associated with surface and ground water end members vary distinctly in most cases and thus, make the hyporheic mixing zone dynamic. As a consequence, a proper understanding of the hyporheic zone entails an understanding of physical, chemical and ecological processes in the hyporheic zone.

.

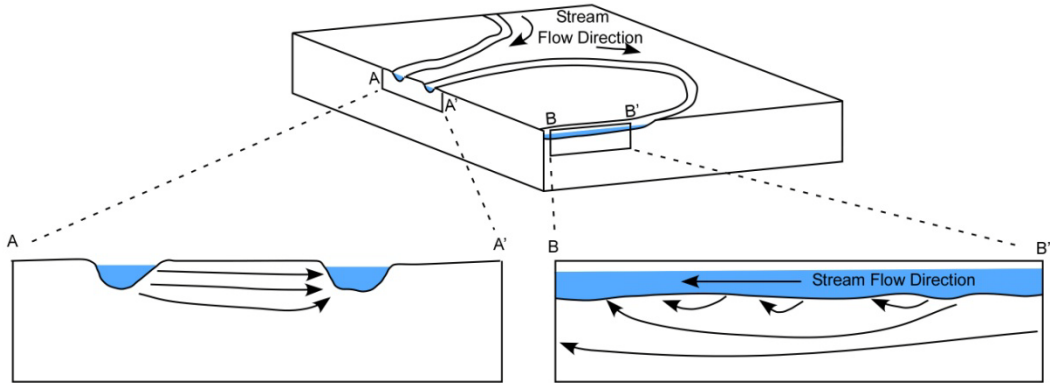

Figure 1 Types of hyporheic flows. A-A' shows transverse hyporheic flow and B-B' shows various extents of longitudinal hyporheic flows.

Significance

Regions of localized ground water upwelling provide year long refugia for fish and other aquatic plants and animals because ground water discharge tends to stabilize flow and moderate the water temperature of streams (Cassie, 1991; Alexander and Cassie, 2003; Anderson 2005). Also, spawning of fish and the growth and development of streambed periphyton are sensitive to water temperatures (Alexander and Cassie, 2003; Cardenas et al., 2008). Stream temperature relies on riparian vegetation, channel width along the length of the stream and most importantly on ground water input. A technique to predict cold stream temperature using the parameters aforementioned was devised using SNTEMP (Stream Network Temperature Model), a model for simulating complex network of streams, as a possible resource for watershed managers to make better decisions to help conserve the brook trout and brown trout population in the Midwest region (Gaffield et al., 2005). Thus, the understanding of temperature patterns in a streambed is important to make better management decisions affecting stream ecology

Statement of the Problem

Although, ground water temperature data and associated tools have been used in a number of applications, their full potential has not yet been utilized. Application of temperature data has been limited to identifying and quantifying seepage (Silliman and Booth, 1993; Silliman et al, 1995; Prudic et al, 2003; Bartolino and Niswonger, 1999; Conlon et al, 2003; Hoffman et al, 2003; Suzuki, 1960) and to determine hydraulic conductivity (Constantz et al, 2003; Bartonilo and Niswonger, 1999; Su et al 2004; Lapham, 1989). Changes in temperature profile within a streambed as a result of seasonal changes are not well studied. Inherent change in thermal and hydraulic properties due to seasonal changes in temperature and changes in biota distribution within the streambed can be expected to cause changes in the temperature profile of the streambed. The study focused on identifying the seasonal changes in hydraulic and thermal parameters and in determining the dominant parameters for respective temperature profiles. In this study, a two dimensional energy transport model, VS2DH, was used to simulate streambed temperatures for weeklong non-storm time periods in spring, summer and winter and to aid the comparison of thermal and hydraulic parameter values between those time periods. The study explored the following two important questions.

1. What is the nature of seasonal change in streambed thermal profile?
2. How do the streambed thermal and hydraulic parameters change over seasons?

Study Area

The study site is a stretch of the Little Kickapoo Creek (LKC), a third-order low-gradient perennial stream, about 15 km south of Illinois State University, adjacent to the university well field. LKC originates in the City of Bloomington and flows mostly

through agricultural fields leading up to the study site (Figure 2). The study site is south of the Bloomington moraine and overlies the poorly-sorted outwash sand and gravel of the Henry Formation. The Henry Formation is 5 to 7m thick and is overlain by about 2m of silt and clay with sand of the Cahokia Alluvium. Clay-rich glacial till of the Wedron Formation underlies the Henry Formation (Figure 3).

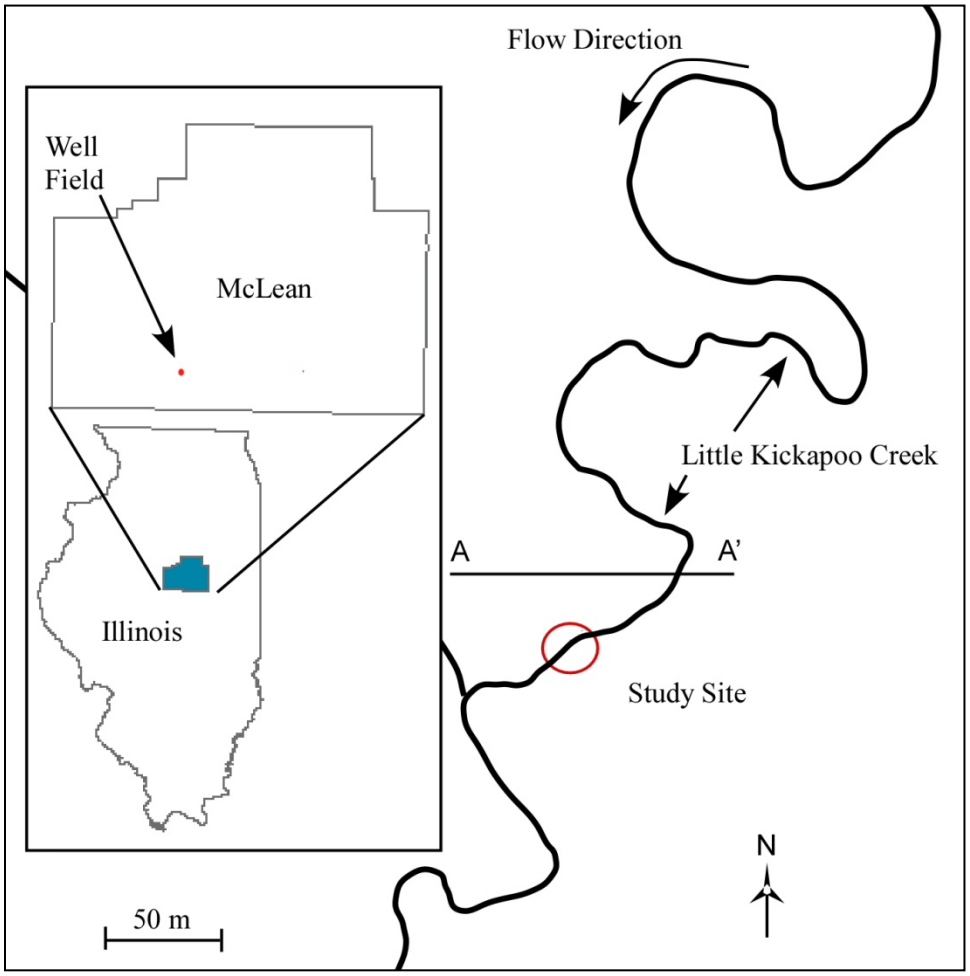

Figure 2 Location of the study site in the Little Kickapoo Creek, Heyworth, IL.

The unsorted sand and gravel of the Henry Formation hosts an unconfined aquifer that is confined in the bottom by the less permeable till of the Wedron Formation. The well field boasts about 50 wells and previous studies have suggested that LKC is well connected with the shallow aquifer (Peterson and Sickbert, 2006). Flowing roughly south, the stream has a gradient of 0.003 and sinuosity index of 1.8 (Peterson and Sickbert, 2006). The discharge ranges from 0.1 $m^3 s^{-1}$ at a mean velocity of 0.05 ms^{-1} to a discharge of greater than 4 $m^3 s^{-1}$ at a mean velocity of 1.2 ms^{-1} (Peterson et al., 2008)

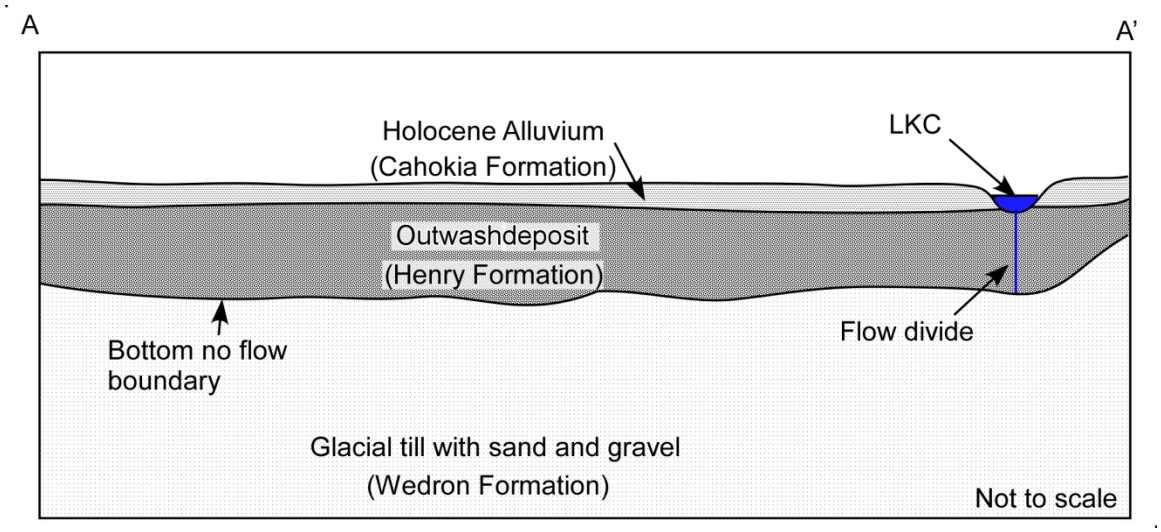

Figure 3 Schematic cross-section for AA' showing the three geologic units.

The study site was selected where meandering was little in order to reduce any effects from hyporheic flow through meander necks (Figure 2). The stream takes a gentle left turn as it approaches the study site. Also, a point bar on the right bank terminates as the stream approaches the study stretch. Sinuosity index for 100m stretch of LKC around the center of the study site is 1.1, that for 200 m stretch of the stream around the center of the study site is 1.4 and regionally the sinuosity index is 1.8. Thus, by selecting a stretch

of the stream that has low sinuosity index locally, we expect to minimize the effect of stream water bypass through meander necks as observed by Peterson and Sickbert (2006) on the streambed temperatures. The stream cuts a narrow channel with steep banks into the top of Henry Formation with a relief of about 2-3m from bank tops to the streambed. The streambed substrate is composed of mostly coarse sand and gravel with interstitial finer sediments and some cobble.

Climate and Precipitation

The area has generally hot wet summers and relatively cold dry winters. Based on average monthly temperatures and precipitation between 1971 and 2000, July and August are the two hottest months with over 22.5°C on average temperatures and January and February are the two coldest months with less than -2.5°C in average temperatures (Table 1). Spring and fall have moderate temperatures. Summer on average receives more precipitation than spring and fall. Average winter precipitation is the least among the seasons. Average monthly precipitation between 1971 and 2000 was highest for May and June with more than 100mm of precipitation and lowest for January and February with more less than 45mm of precipitation. In 2009, April received over 150 mm of precipitation. Precipitation for July was over 90 mm and that for August was over 120mm. Monthly precipitation for Jan of 2010 was less than 40mm and makes up for one of the driest months during the study period.

Table 1 Average monthly precipitation and temperatures near the study site.

	Jan	Feb	Mar	Apr	May	Jun	Jul	Aug	Sep	Oct	Nov	Dec
Average Precipitation (mm)												
1971-2000 [b]	38.6	42.4	76.5	90.9	108.5	101.3	95.8	93.0	84.6	66.3	81.5	73.4
2009 [b]	3.3	31.2	117.9	155.2	134.4	193.3	90.2	121.7	45.5	263.7	78.7	93.0
2010 [a]	38.6											
Average Temperature (°C)												
1971-2000 [a]	-5.3	-2.6	3.7	10.3	16.6	22.1	24.0	22.9	18.7	12.1	4.3	-2.2

Data adapted from Water and Atmospheric Resources Monitoring Program (2010) and NOAA (2010).

[a] Data collected at Normal 4NE station.

[b] Data collected at Bloomington Works station.

CHAPTER II

METHOD

A series of field, lab, and computational methods were used while answering the research question. Hyporheic wells equipped with temperature loggers and sampling tubes were used to record streambed temperatures and to collect samples during the bromide test. The tracer test was done using sodium bromide solution and fed to LKC upstream while samples were collected in the wells downstream. The tracer test provided valuable information on the nature of hyporheic flow. Loggers installed in the stream and a piezometer collected temperature data for the surface water and ground water. Preliminary analysis and subsequent data reduction to time periods of interest were done in a spreadsheet software. Numerical modeling was done with VS2DH, a USGS energy transport model. Programs written in MATLAB were used for error analysis of the models and for file handling.

Hyporheic Wells and Piezometers

Six hyporheic wells made up of 3.81 cm PVC pipes were installed in the thalweg at an interval of 5m (Figure 4). The wells were emplaced by inserting them inside drive point well casing made of 5.08cm galvanized pipes and later removing the casing. Each hyporheic well was installed with temperature loggers and sampling pipes at depths of 30 cm, 60 cm, 90 cm and 150 cm as shown in Figure 5. Holes were drilled at corresponding depths to allow for thermal equilibrium with the surrounding sediment and to allow

subsurface water sampling from those depths. The loggers and sampling points were separated using foam sealant.

Data Collection

Temperature loggers used included StoyAway TidbiT Temperature Loggers (Accuracy: ±0.2°C (0.4°F) at 70°F; Resolution: 0.16°C (0.29°F) at 70°F), HOBO® Pendant Temperature and Light Data Loggers (Accuracy: ±0.47°C (±0.85°F) at 25°C (77°F); Resolution: 0.10°C (0.18°F) at 25°C (77°F)) and HOBO® Pendant Temperature Data Loggers (Accuracy: 0.47°C (0.85°F) at 25°C (77°F); Resolution: 0.10°C (0.18°F). The loggers were setup to record temperature at 15 min interval to allow for sufficient temporal resolution and to ensure that the samples recorded were within the storage capacity of the loggers.

Data was collected from February 2009 to March 2010. The first set of wells was installed in February of 2009 and included 5 hyporheic wells and 1 stilling well. Two temperature loggers were also installed to measure stream temperatures and one temperature logger in an adjacent deep well to measure deeper ground water temperature. Installation of Well 6 was done in May. The first set of wells and stream temperature loggers were retrieved starting late August while replacing them with second set of wells and loggers. The second set of wells and loggers were retrieved in early March of 2010.

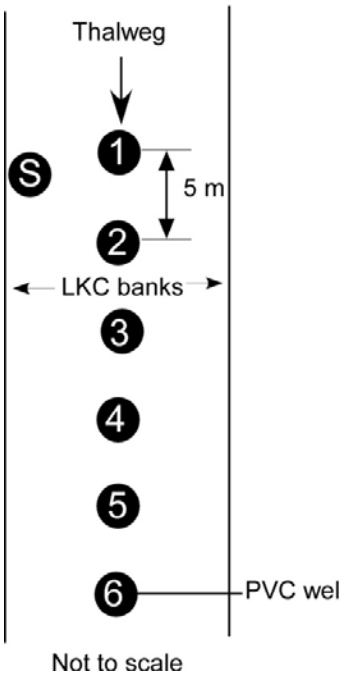

Figure 4 Schematic setup of hyporheic wells (1-6) and stilling well (S) in the study site.

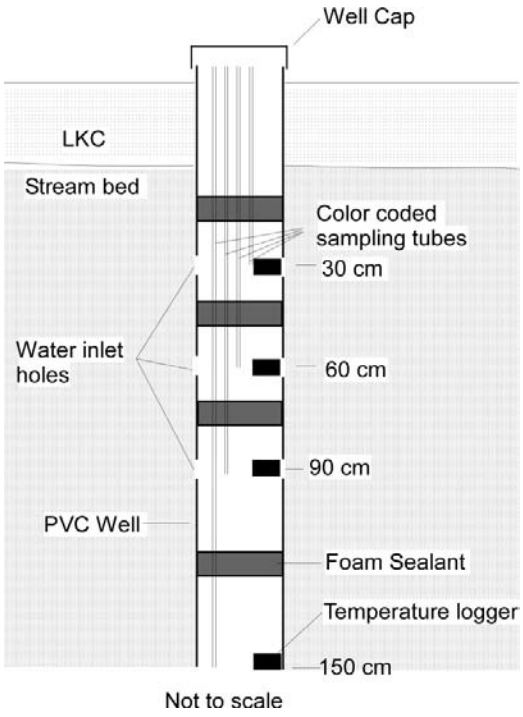

Figure 5 Design of individual hyporheic wells.

Data collected at the site were initially analyzed to identify any problems in data collection and to select appropriate time periods for thermal modeling. Stage data, collected using Solinst Levelogger® installed in the stilling well, were used to select week long periods in spring, winter, and summer that did not have storm events. Hyporheic zone and the thermal regime of the streambed behave differently between storm events and standard flow (Oware, 2010), and it is thus, necessary to avoid the effects of storm events in the streambed to successfully study seasonal changes in thermal profile of the streambed. Boundary conditions for temperatures at depths of 30, 60, 90 and 150 cm, stream temperatures and ground water temperatures were fed to the models in at 4 hour intervals.

Scour and Fill

Scour and fill can be expected to affect thermal interactions in the streambed because these events bring about changes in the streambed material and thickness. A simple rod and sliding washer method was used to measure scour and fill events. Four markers were installed in May between each well bracketed by Well 2 and Well 6 and periodic measurements were taken to determine the depth to the streambed and to the washer from the marker top. During scour events the washer would slide down the marker rods to the depth where streambed entrainment takes place. During fill events the washer will be covered by additional streambed sediment. And by subtracting the previous depth to the streambed from the current depth to the washer, the amount of scour can be identified. Fill following the scour event can be determined by calculating the difference between current streambed level and current bead level. Scour and fill marker reading were recorded between May and October of 2009. The washers were reset to the current streambed level at the end of each field measurement.

Tracer Test

A bromide (Br^-) tracer test was performed using NaBr in August in order to identify hyporheic flow patterns in the streambed. 300 gallon solution was prepared using 12 kg of NaBr and was gravity fed to the stream about 15m upstream of Well 1 using a perforated injection tube to allow for an even distribution in the stream. Water samples were taken in 10 min intervals in the beginning and in 15 min intervals in the latter part of the injection period using Masterflex E/S Portable Samplers. The injection took 2 hours 50 min after which samples were collected every 30mins and hourly from 6 hour until 15 hour into the tracer test. Final samples were taken at 24 hours since the injection began. The samples were analyzed using Dionex DX-120 ion chromatograph for

bromide. The extent of hyporheic zone extent in the streambed was then studied by identifying the depth where bromide concentration is 10% of the bromide concentration in the stream (Note: Br^- concentration in ground water was zero). The method suggested a hyporheic zone extent of less than 1m from the streambed surface. Streambed around wells 1, 3 and 6 likely had a hyporheic extent of less than 20 cm. Tracer tests were not performed for winter or summer time period.

Thermal Modeling

VS2DH is a two dimensional heat and ground water flow simulation model built from modifications to VS2DT, a solute transport model developed by the USGS (Healy and Ronan, 1996).VS2DH simulates energy transport in a variably saturated porous medium and assumes a single, constant-density liquid phase flow and is well suited to simulate applications where vapor-phase flow and fluid density variations are negligible. The model makes use of the finite difference method to solve the advection-dispersion equation (Equation 1) and provides a user friendly interface with the help of a graphical software VS2DHI.

$$\frac{\partial}{\partial t}[\theta C_w + (1-\varphi)\, C_s\,]T = \nabla \cdot K_T(\theta)\nabla T + \nabla \cdot \theta C_w D_H \nabla T - \nabla \theta C_w\, vT + qC_w\, T^* \qquad (1)$$

where θ is volumetric moisture content, φ is porosity, C_w is heat capacity of water, C_s is heat capacity of dry solid, T is temperature, K_T is thermal conductivity of water and solid matrix, D_H is coefficient of hydrodynamic dispersion, q is rate of fluid source and T^* is temperature of fluid source or sink. The terms on the right hand side represent heat change in the system due to conduction, dispersion, advection and sink or source respectively.

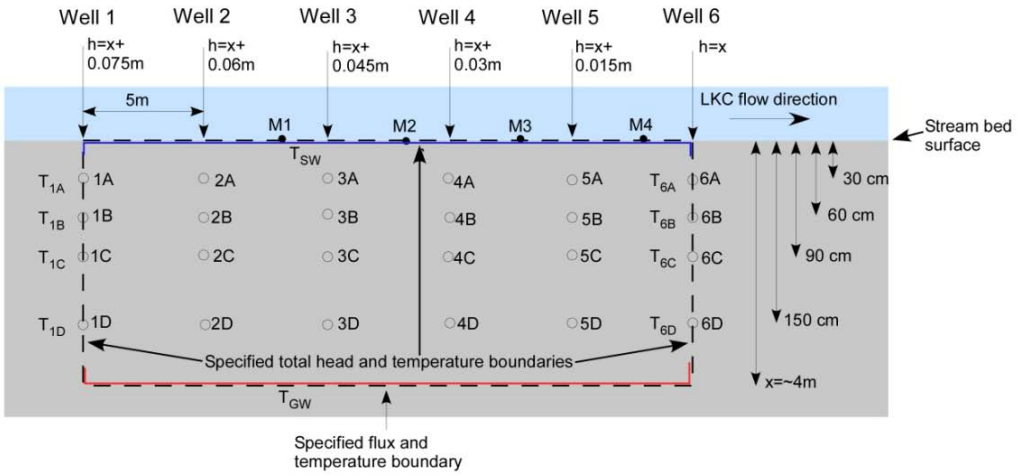

Figure 6 Conceptual model of the streambed showing location of the temperature loggers. Dash lines represent the extent of the domain used in the numerical model.

Thermal modeling was based on the conceptual model that assumed a homogeneous medium with a gradient of 0.003 as shown in Figure 6. Boundary conditions were fed into the model every four hours. The temperature data from Well 1 and Well 6 were used as boundary conditions for the thermal models. Temperatures from wells 2 through 5 were used to specify the initial temperature contours in the model. Streambed topography changes represented by the scour and fill data were used to define the top of the domain. Total head values decreased at 0.015m for every 5m change in distance in the downstream direction. Thermal boundary conditions of the upper and lower boundary of the domain were defined by the temperature of the stream and ground water respectively. Also, the thermal boundary conditions for the left and right boundaries were defined by the temperature recorded by the loggers at various depths. Hydraulic properties of medium sand provided by VS2DH were initially used in the models. Parameter values available in the literature were used to specify the thermal parameter values. Table 1 summarizes the range of parameter values of selected material

and the values initially used in the models prior to model optimization. The model was set up to give output values every 15 minutes thus enabling comparison with the observed values at the same scale.

Table 2 Representative value ranges for hydraulic and thermal parameters.

Parameter		Value Range	Initial values for models
Horizontal Hydraulic Conductivity (m s^{-1})			4.63×10^{-3}
	Fine sand	2×10^{-7}-2×10^{-4} [a]	
	Coarse sand	9×10^{-7}-6×10^{-3} [a]	
	Gravel	3×10^{-4}-3×10^{-2} [a]	
Heat Capacity ($Jm^{-3}°C^{-1}$)			
	Dry Solid	1.1×10^{6}-1.3×10^{6} [a]	1.2×10^{6}
	Water	4.2×10^{6} [a]	4.2×10^{6}
	Saturated Solid	2.5×10^{6}-3.2×10^{6} [a]	
Porosity			0.375
	Sand	0.25-0.50 [a]	
	Sand and gravel	0.15-0.35 [a]	
Dispersivity (m)		---	0.005
Vertical Anisotropy (Kh/Kz)			10
	Sand and gravel	3-5 [b]	
	Fine/medium sand	10-30 [b]	
	Fine sand and silt	30-100 [b]	
Saturated Thermal Conductivity ($W m^{-1}°C^{-1}$)			2.1
	Saturated sediments (sand, loam, etc.)	1.4-2.2 [a]	
	Average saturated soil	2.9 [a]	

[a] Values adapted from Weight (2008)
[b] Values adapted from Masterson et al. (2007)

Thermal modeling was firstly done for the first week in April. Due to the lack of data for Well 6, temperature from Well 1 was used for Well 6 boundary conditions. The affects of this substitution in the model should be negligible because of the downstream location of the Well 6. The lower hydraulic head at Well 6 causes the horizontal component of ground water flux to move out of the domain. In such advective conditions

the boundary condition in the downstream side of the domain is expected to have less influence in the temperature profile in the upstream direction. In addition, the average temperature difference between Well 1 and Well 5 during the time period, at 0.38°C, was within the accuracy of the loggers. Model optimization was based on reducing the mean absolute error (MAE) model by making proper adjustments to parameters on a trial and error basis. MAEs were calculated using a program written in MATLAB (Appendix C). MAE graphs were constructed for each parameter and the parameter value associated with the vertex of the error curve was picked within the range of plausible values. The models were adjusted for base flux, followed by adjustments to horizontal hydraulic conductivity, saturated thermal conductivity, dry heat capacity of the medium, vertical to horizontal conductivity ratio, and porosity until the best fit model for the time period was obtained. Best fit models were similarly obtained for summer and winter model weeks. Finally, the changes in thermal profiles were compared between the three models using the depth of the surface-temperature front, changes in thermal and hydraulic parameters and changes in sensitivity of these parameters.

Sensitivity analysis was done by creating MAE graphs for all the parameters at fixed percent increments from the original parameter value. More often than not model improvement occurred while attempting a sensitivity analysis. In such cases, parameter values were corrected before creating another set of MAE graphs. The process continued until the best fit model gave least error for all the parameters.

CHAPTER III

RESULTS

Stream water temperature fits a yearly sinusoidal curve with diurnal sinusoidal temperature imprinted on it as shown in Figure 7. Yearly temperature range of about 30°C was observed with highest temperatures observed between June and August, and lowest temperatures observed between December and February. This pattern closely follows the air temperature patterns from Table 1. Stream stage was relatively higher in spring and winter compared to summer and fall. The site was subjected to a series of storm events with periods of recovery between the storm events. Recovery periods in winter from storm events to base flow were longer in winter compared to spring or fall. Despite the higher average precipitation in summer storm events were smaller compared to spring, fall and winter. Week long periods in spring (April 1-7, 2009), summer (Jul 27-Aug 2) and winter (Jan 15-21) were selected where storm events are small or absent and will be referred to as *the spring*, *the summer*, and *the winter* model periods hereafter. Stream temperature was on average about 8°C during the spring model period and about 22°C and 2°C during the summer and winter model periods respectively (Table 3). The temperature of ground water, however, remained around 11°C throughout the model periods with subtle changes over the seasons. Lowest ground water temperatures were seen in early June and peaked around December with a lag time of about 6 months.

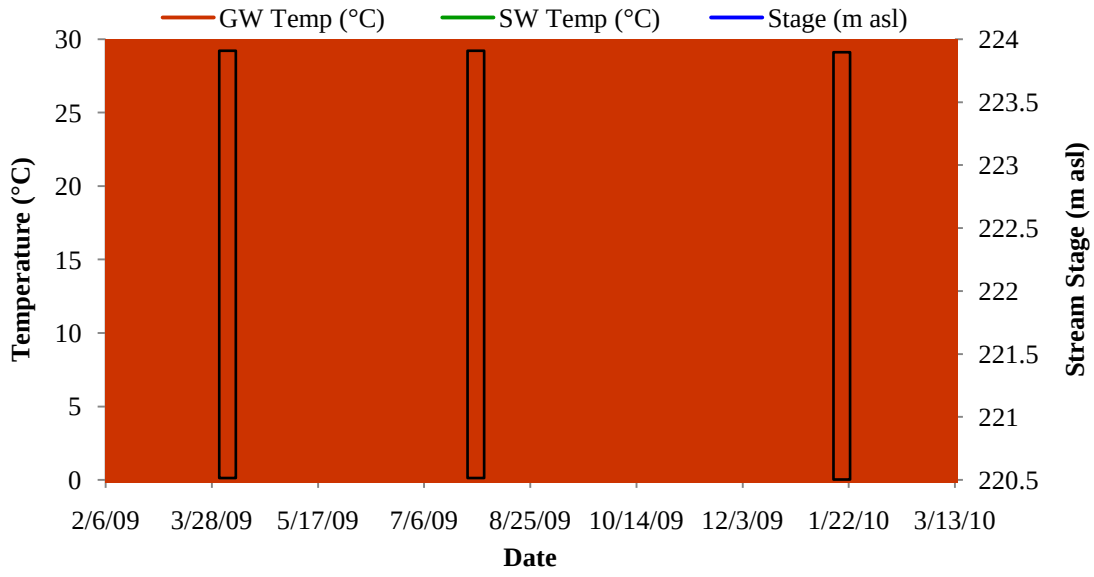

Figure 7 Graph showing stream stage, ground water and stream temperatures over the period of data collection.

Table 3 Average temperature ranges and averages for the three model periods.

	Spring model week		Summer model week		Winter model week	
	Range (°C)	Avg (°C)	Range (°C)	Avg (°C)	Range (°C)	Avg (°C)
Surface water	6.59	8.22±1.63	7.96	22.13±2.02	2.81	2.03±0.63
30 cm	0.69	8.63±0.20	1.22	18.26±0.28	0.53	6.12±0.15
60 cm	0.46	9.34±0.08	0.33	16.49±0.09	0.27	7.57±0.08
90 cm	0.25	9.40±0.04	0.24	15.26±0.09	0.13	8.47±0.03
150 cm	0.05	9.59±0.03	0.34	13.46±0.09	0.14	9.51±0.05
Ground water	0.31	11.26±0.07	0	10.96	0	11.73

During the spring model period ground water is on average 3°C higher than surface water. Diurnal fluctuations give the week a stream temperature range of about 6°C. Streambed temperature fluctuations drastically decreased to about 0.7°C for 30 cm depth and to less than 0.3°C at 90 cm depth (Table 3). There are two small storm events during the week long period. These storm events cause some alteration in the diurnal

fluctuations of stream temperatures and the effect of second storm event is more noticeable with a subdued peak on day 6 (Figure 8). These storms also cause slight error spikes in the model as will be shown later in the section (Figure 16). A major storm event occurred about 3 weeks before the spring model period. The possible effect of these storm events on streambed will later be discussed.

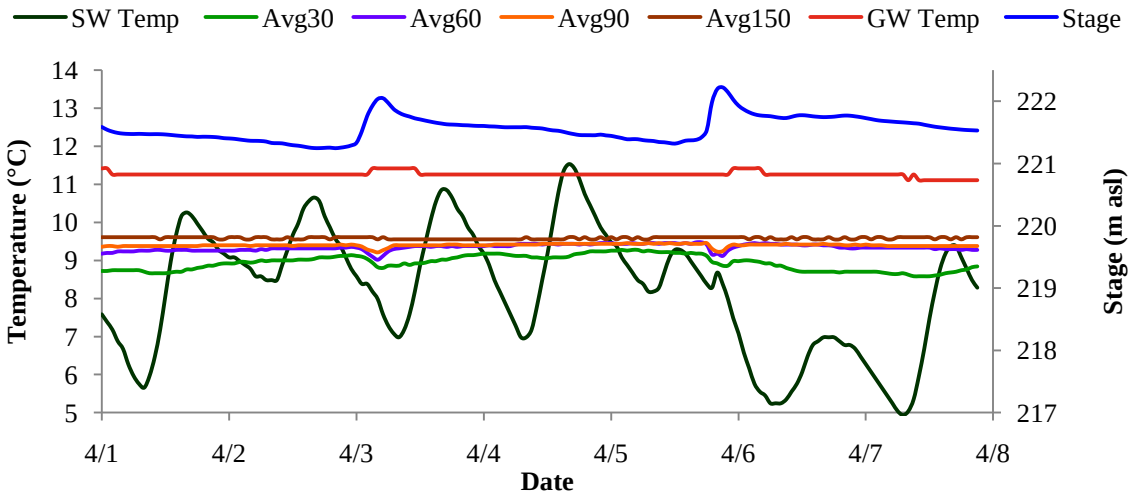

Figure 8 Stage, surface and subsurface temperatures during the spring model week.

The summer model period has the stream water on average 11°C higher than the ground water. Subsurface temperature fluctuations of over 1.2°C were observed at 30 cm depth and about 0.3°C at 150 cm depth. While ground water temperature remains steady, stream temperatures experiences a strong diurnal fluctuations and shows a weekly temperature range of about 8°C with an average temperature of about 22°C. Average temperature inflection was observed at 90 cm. The stream maintains a low flow without any storms during the period (Figure 9). Ground water temperatures remain steady during

the period. A major storm event occurred about five weeks before the summer model period.

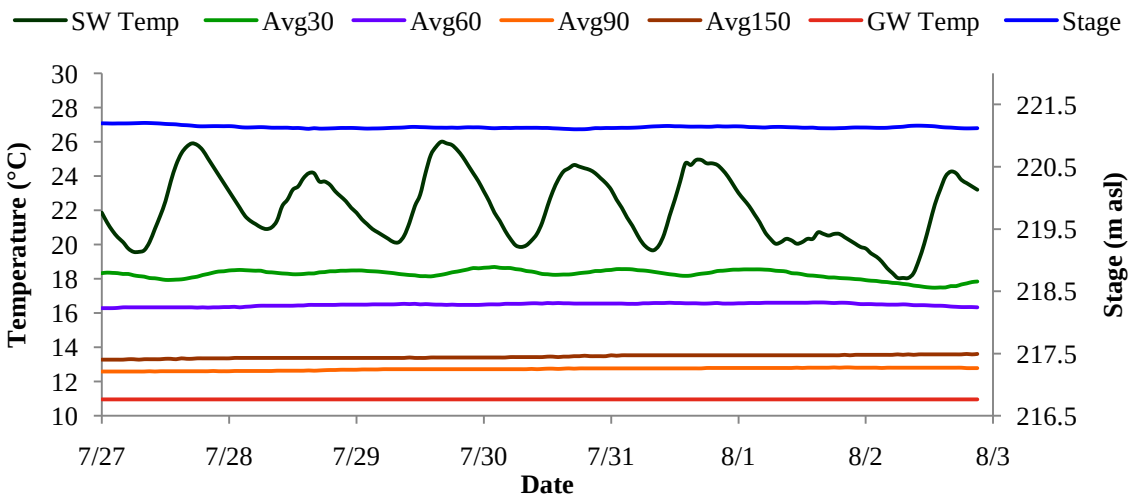

Figure 9 Stage, surface and subsurface temperatures during the summer model week.

During the winter time period, the stream temperature is near zero and diurnal fluctuations are weak with weekly temperature range of 2°C. Ground water temperatures are on average about 10 °C higher than the stream temperatures (Figure 10). Sub-surface temperature fluctuations in the subsurface are comparatively smaller than the summer model week with fluctuations of about 0.5°C at 30 cm and of less than 0.15°C at 90 cm depth. Average temperature inflection was observed at 30 cm depth. No storm events were seen during this time period. However, a major storm event occurred about three weeks before.

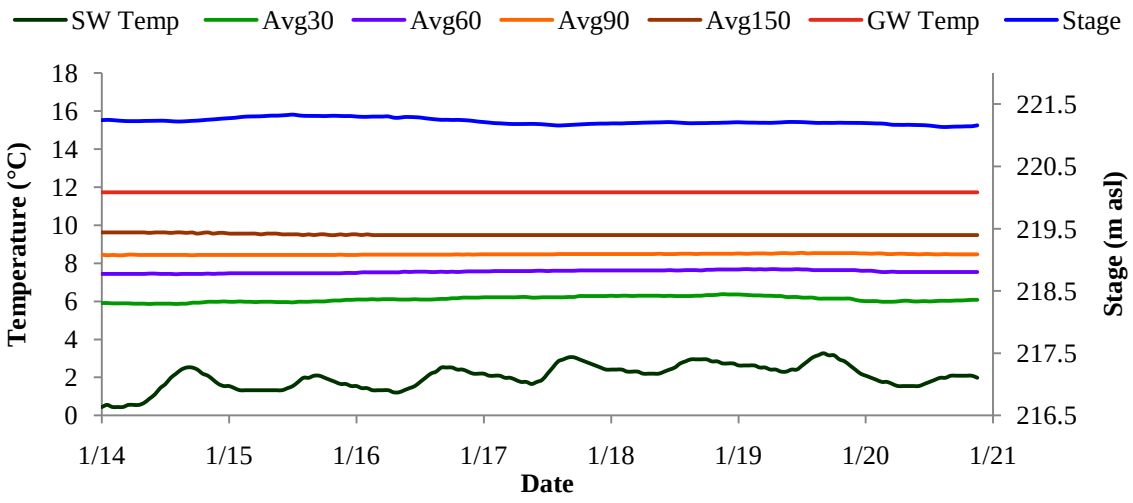

Figure 10 Stage, surface and subsurface temperatures during the spring model week.

Streambed Topography

Parts of two riffle and pool sequence were observed in the study stretch. Well 1 was located in the upstream riffle while Marker 3 is located in the downstream riffle as shown in Figure 11. Well 2, 3 and 4 were located in the upstream pool. Well 5 and 6 are located in the downstream pool. Studies on the dynamics of riffle and pools have suggested that hyporheic flows enter the streambed at the downstream end of a pool and emerge on the upstream end of the next pool (Harvery and Bencala, 1993, Winter et al., 1998). As a result, stream water can be expected to flow into the substrate in Well 3 and 4 and emerge in Well 4 and 5. No major change in the position of riffles and pools was observed over the period of the study.

Scour and fill data showed scour events of up to 10 cm suggesting streambed mobilization during the storm events. Much of these scours were subsequently filled at the end of the storm events as represented by the fill values (Appendix A). Over the period of about 9 months elevation changes of up to 20 cm occurred between the highest

and lowest elevation points along the stretch of the stream (Figure 11). Lowest elevation profile was observed during the installation of the wells in February and the highest elevation profile was observed in May. Most of the sediment added to the streambed was between February and May; part of which was eroded in the consecutive months.

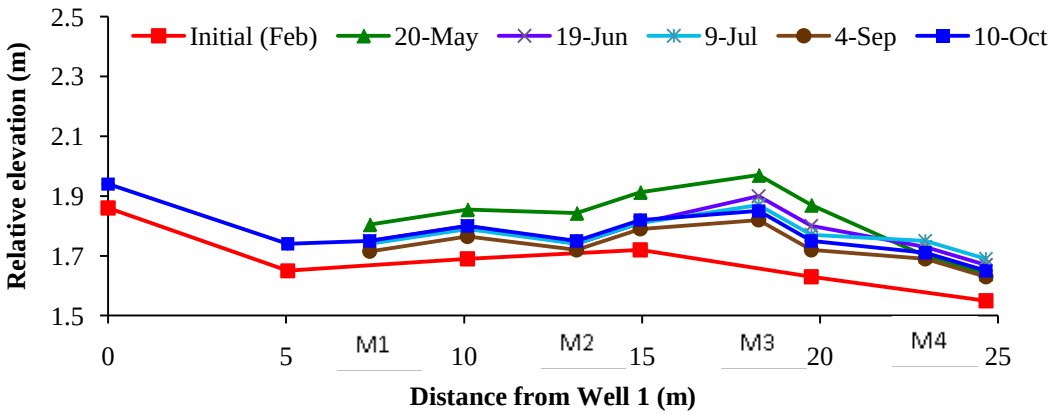

Figure 11 Streambed profile changes from February to October.

Tracer Test

Bromide discharge into the stream resulted in little influence on streambed bromide concentration. Overall concentration of bromide decreased with depth with almost no bromide at 90cm and 150cm depths (Appendix B) confirming that stream is a gaining stream and local hyporheic flow has shallow penetration into the streambed subsurface during the period of the tracer test. Comparatively large concentrations of bromide were detected within a small lag period in sample points 2A and to a lesser extent in 4A as shown in Figure 12. Higher concentrations of Br^- in 2A suggest that more stream water in introduced to the streambed around Well 2 than other wells. The

hyporheic zone in the streambed extended to depths of 30-80 cm delineated by Br^- concentrations that are 10% of Br^- concentration in the stream.

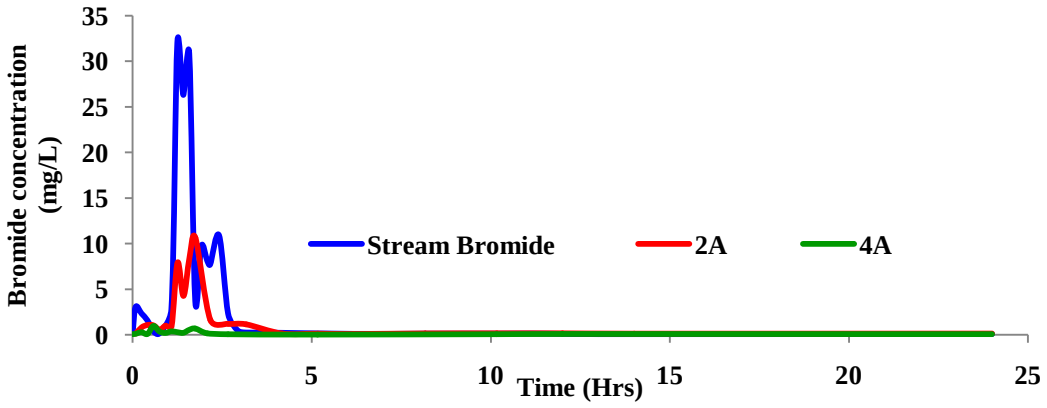

Figure 12 Bromide concentrations for sample points with higher concentrations of bromide.

Temperature Models

One of the most obvious differences represented by the simulated models is the difference in thermal gradient in the three model periods (Figure 13-Figure 15). A low thermal gradient with temperature difference of 3°C between surface and ground water was observed for the spring time period while comparatively large gradients with temperature differences of about 11°C and 10°C were observed for the summer and winter time periods. A reversal of thermal gradient occurred from the winter model to the summer model with the ground water at low thermal potential during the summer time period and the surface water at low thermal potential during the winter time period. The temperature of ground water remained fairly constant at around 11°C throughout the model periods. The models simulated stream induced hyporheic flow into the streambed

across upper boundaries where boundary conditions in total head change. Stream induced temperature fluctuations, were limited to the shallow substrate in all three models.

Temperature fronts in the streambed can be looked at in terms of temperatures in the streambed that are some percentiles of the temperature distribution. The median average temperature (MAT) value for each model week was calculated and outlined in the model outputs from VS2DH. The relative changes in MAT between the three model periods were compared. MAT front for the spring time period was relatively deeper compared to those of summer and winter time periods while that of winter time period was the shallowest. Since, heat is not a conservative tracer, these temperature fronts cannot be used to accurately quantify the extent of hyporheic flows. However, in shallow streambeds it allows for a comparison of the effect of stream water on shallow streambed temperatures.

A relatively low model error was obtained for the spring time period with a MAE of 0.2°C compared to MAE of 0.4°C and 0.3°C for the summer and winter time periods (Table 4). The MAEs for all three models are comparable to the range of logger accuracy i.e. 0.2-0.47 °C. Lower observed temperature compared to the simulated temperature at 60 cm depth of Well 4 and the model's inability to represent daily fluctuations in temperature at 30 cm depth seems to have contributed to the MAE for the summer model (Figure 17). Similar difficulty in representing temperatures at 30 cm depth can also be observed to some extent in spring and winter modes. Lower observed temperature compared to simulated temperature at 30 and 60 cm of Well 2 (Figure 18) contributes to the higher MAE for the winter model.

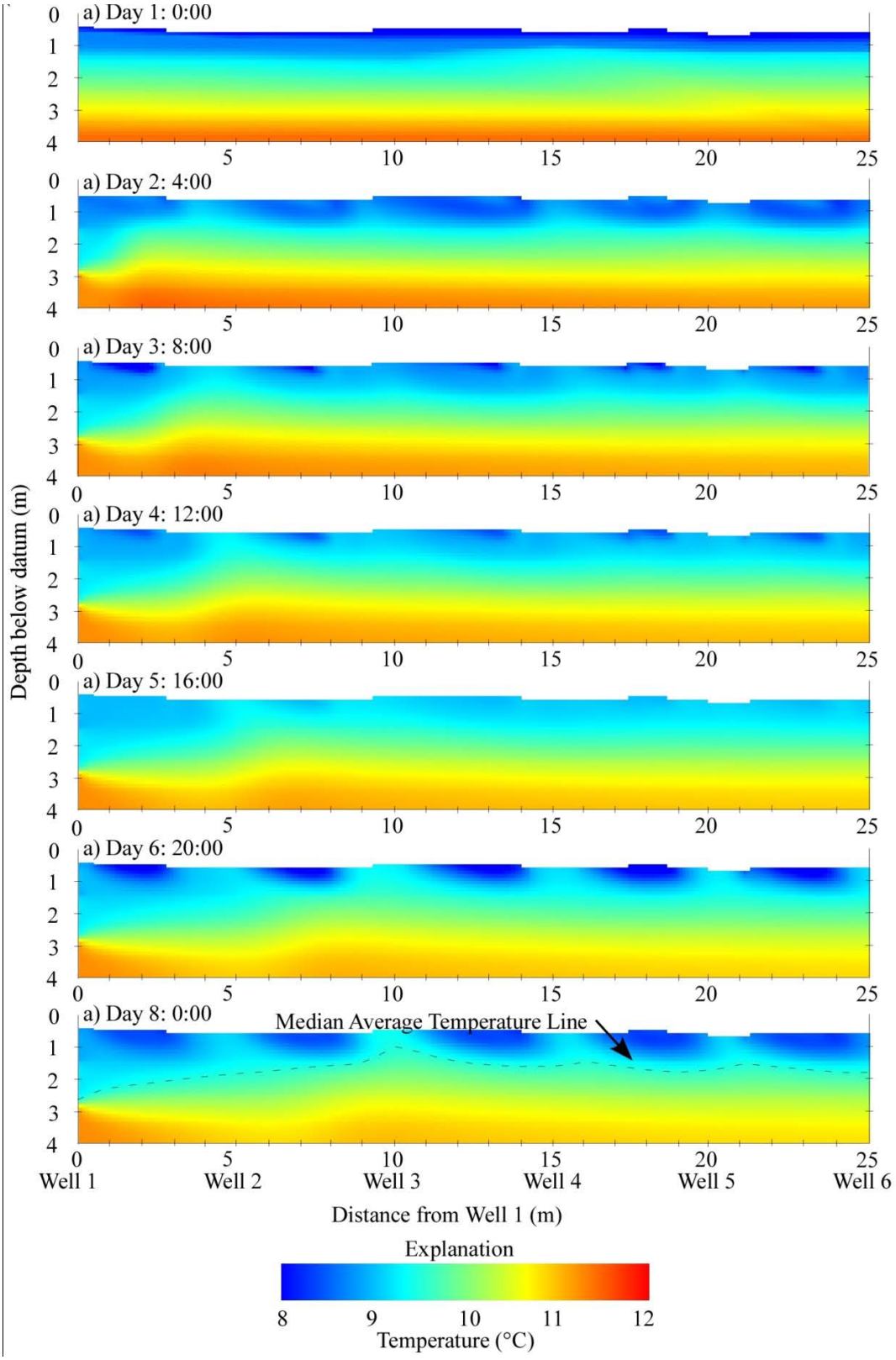

Figure 13 Best fit VS2DH models simulating streambed temperature distribution for the spring model period.

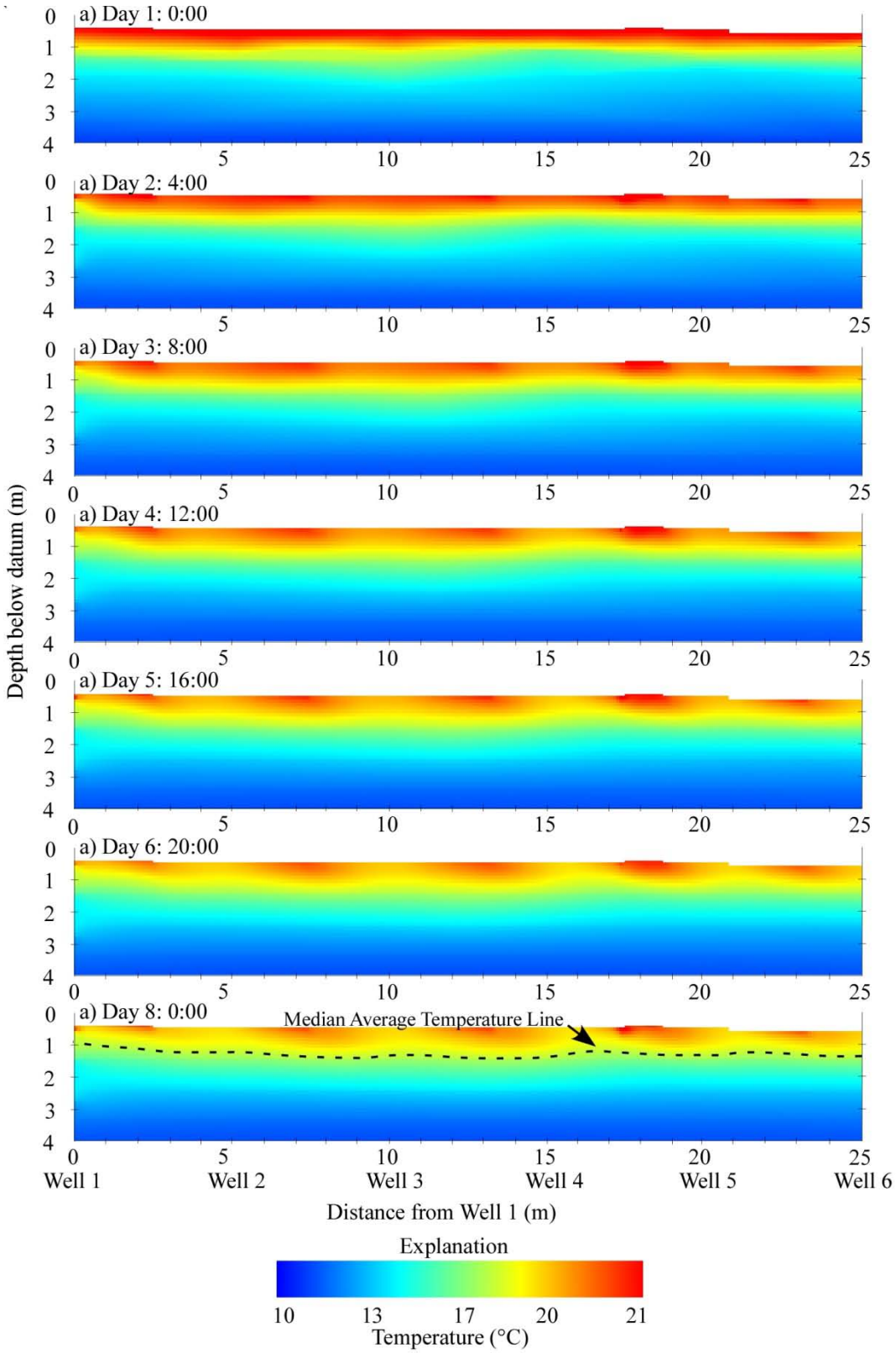

Figure 14 Best fit VS2DH models simulating streambed temperature distribution for the summer model period.

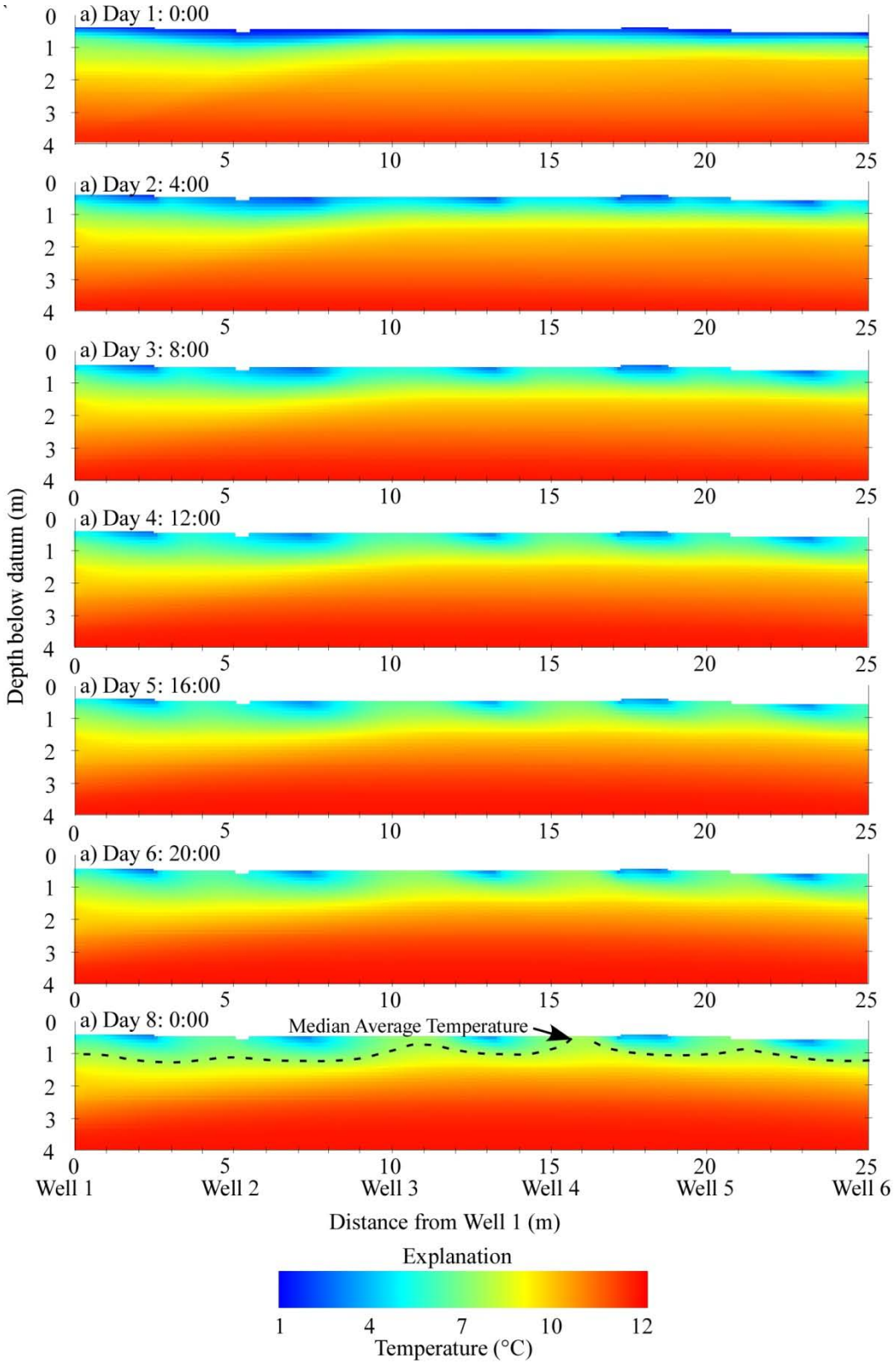

Figure 15 Best fit VS2DH models simulating streambed temperature distribution for the winter model period.

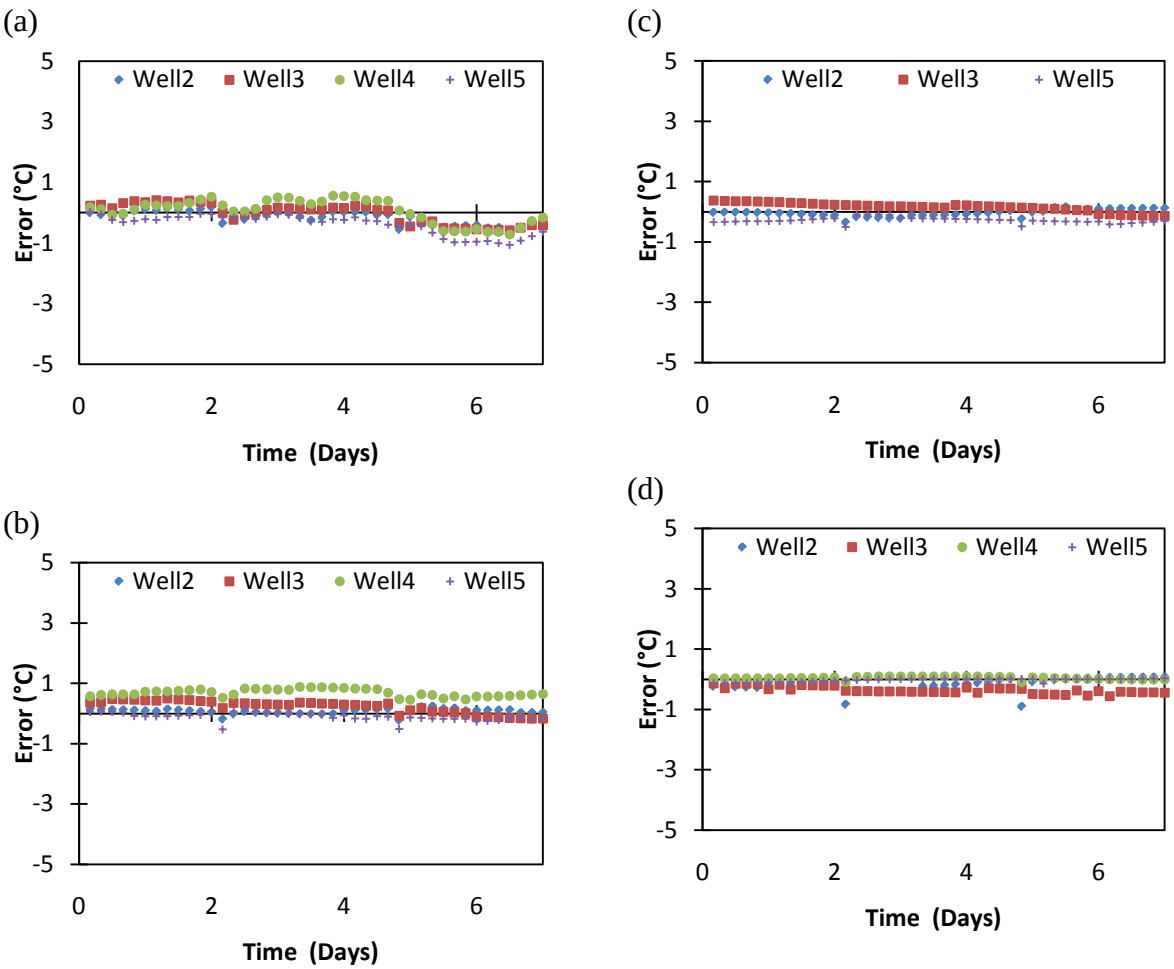

Figure 16 Error graphs for the spring time period at depths of a) 30 cm, b) 60 cm, c) 90 cm and d) 150 cm.

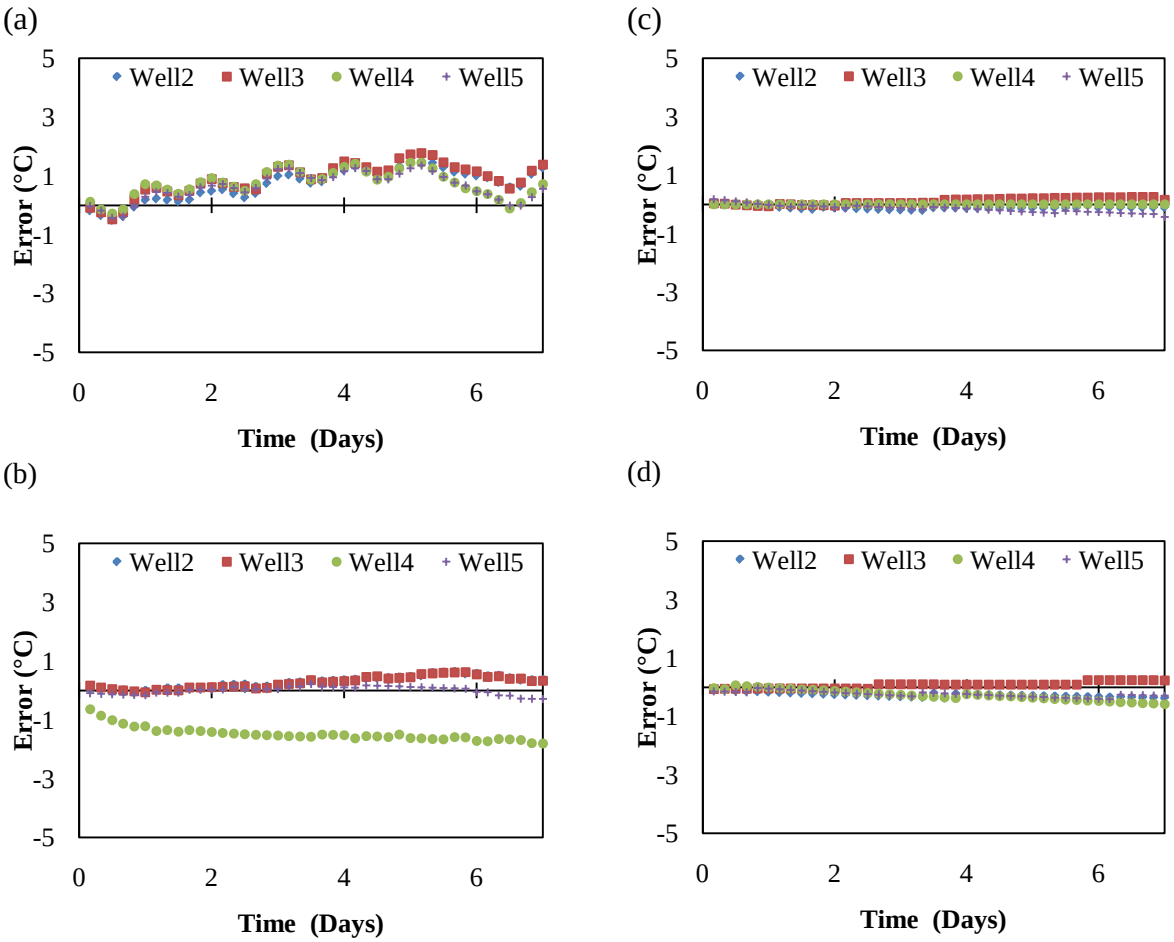

Figure 17 Error graphs for the summer time period at depths of a) 30 cm, b) 60 cm, c) 90 cm and d) 150 cm.

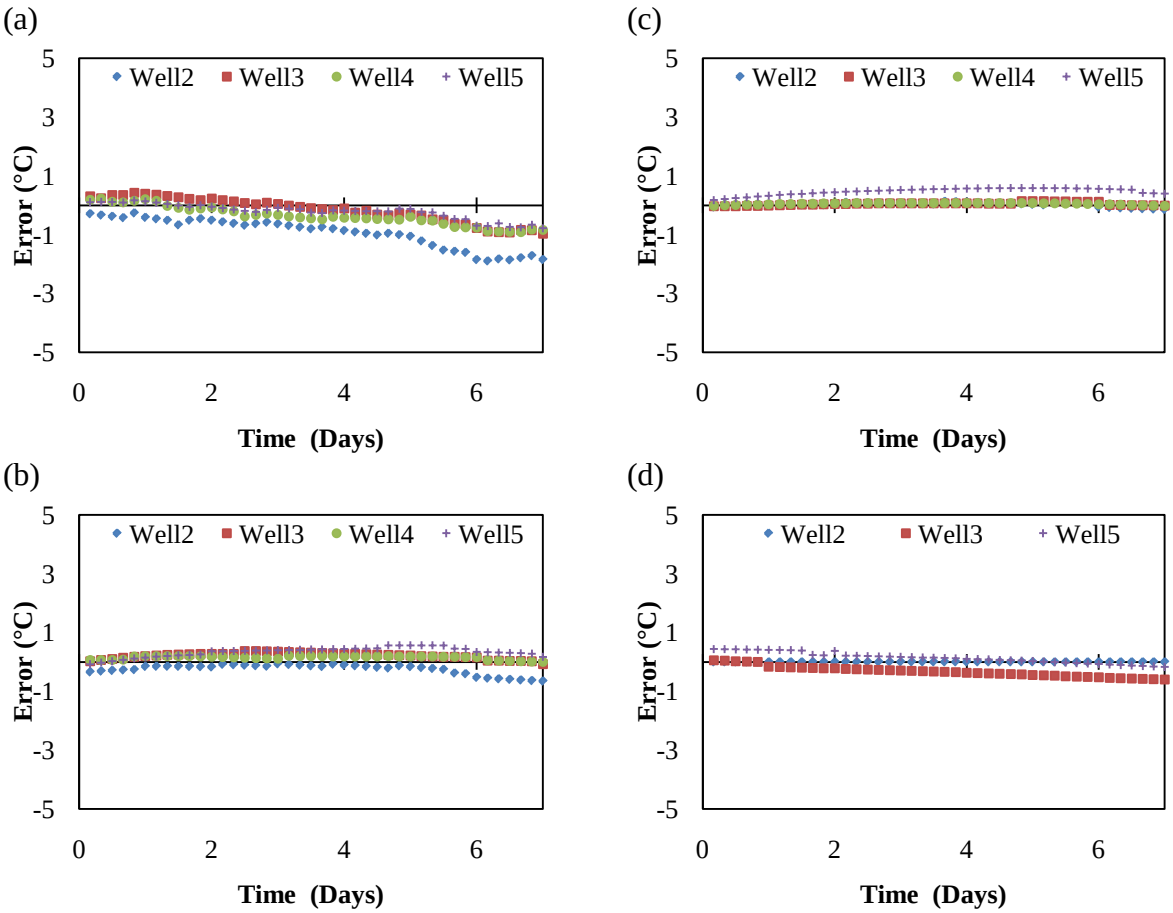

Figure 18 Error graphs for the winter time period at depths of a) 30 cm, b) 60 cm, c) 90 cm and d) 150 cm.

The thermal models, despite some pockets of comparatively higher errors, do a good job of simulating the observed temperatures (Figure 19). Simulated temperatures represent the temperatures better for deeper observation points. Relatively larger deviations from observed temperatures are seen at 30 cm depth. It should be noted that for the spring model, the range of temperatures is narrow and the overlapping of simulated temperatures are likely a result of similar temperatures across the depth of the streambed.

a)

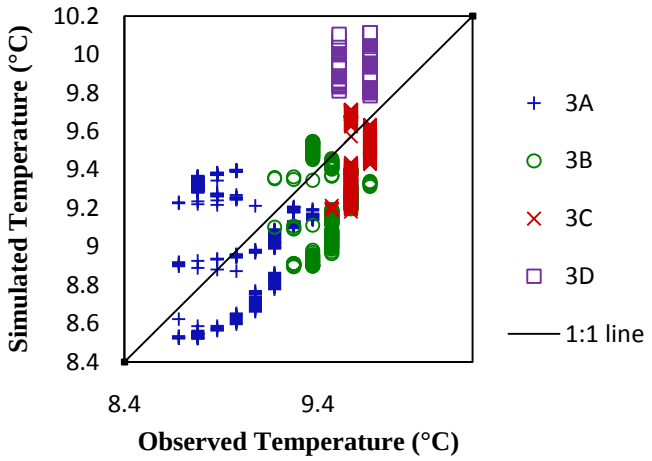

b)

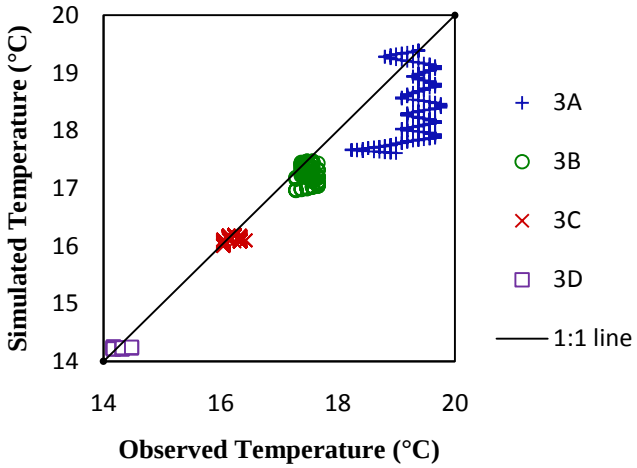

c)

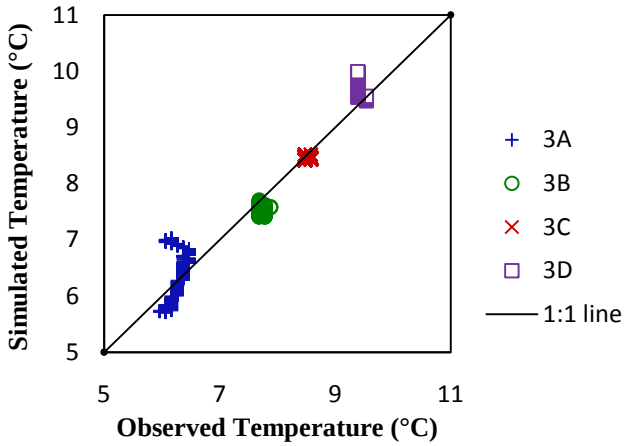

Figure 19 Comparison of observed and simulated temperature for Well 3 for spring, summer and winter model periods a)-c) respectively.

Parameter Values and Sensitivity Analysis

Comparison of parameters from the best fit spring, summer and winter time periods suggest some changes in these parameters between the models. It is however important to take into account the sensitivity of these parameters before making interpretations. Vertical flux of over 2 x 10^{-6} m s^{-1} was seen for the winter model period while fluxes of 1.5 x 10^{-7} m s^{-1} and 7.58 x 10^{-7} m s^{-1} for spring and summer model periods resulted in the best fit model (Table 4). Hydraulic conductivity values were highest for spring model at 2.8 x 10^{-3} m s^{-1} and lowest for the summer model with a value of 1.1 x 10^{-3} m s^{-1}. Saturated thermal conductivity and dry heat capacity values have a narrow range in earth materials and are not expected to change significantly over seasons. As a result, adjustments to these values were halted if the model values exceeded the range of accepted values. The models optimized for vertical anisotropy value of 100 for summer and values less than 30 for spring and winter. A high value for porosity was seen for the best fit summer model.

Table 4 Parameter values for the best fit models for the spring, summer and winter time periods.

Parameter	**Spring**	**Summer**	**Winter**
Vertical flux (m s^{-1})	1.5 x 10^{-7}	7.58 x 10^{-7}	2.3 x 10^{-6}
Horizontal Hydraulic Conductivity (m s^{-1})	2.8 x 10^{-3}	1.1 x 10^{-3}	2.0 x 10^{-3}
Sat. Thermal conductivity (W m^{-1} K^{-1})	2.51†	1.38*	1.38*
Dry heat capacity (J m^{-3} K^{-1})	1.1 x 10^{6*}	1.3 x $10^{6\dagger}$	1.3 x $10^{6\dagger}$
Kh/Kz	9.1	100†	28
Porosity	0.22	0.5†	0.5†
MAE (°C)	0.2	0.4	0.3

* indicates that the parameter value was the lowest value used.

† indicates that the parameter value was the highest value used.

Sensitivity of the models to the various thermal and hydraulic parameters changed from one model period to another. A proper understanding of the sensitivity of the model to these parameters is critical in making proper interpretation of the parameter values. Let us take a look at similarities and differences in sensitivities of the model to the various parameters for the three models.

The spring model sensitivity was very small compared to the accuracy of the loggers used with MAE changes of less than 0.03°C with 50% change in parameter values of the best fit model. No change in MAE was observed with changes in lower values of Kh for the summer and winter models. However, a 50 % increase in Kh resulted in a MAE increase of 0.05°C for the summer model. The summer model showed some of the highest sensitivities to lower values of porosity and higher values of thermal conductivity with MAE changes of over 0.1°C with 50% change in the parameter values. Comparable sensitivities were observed for vertical flux and anisotropy in the winter model.

a)

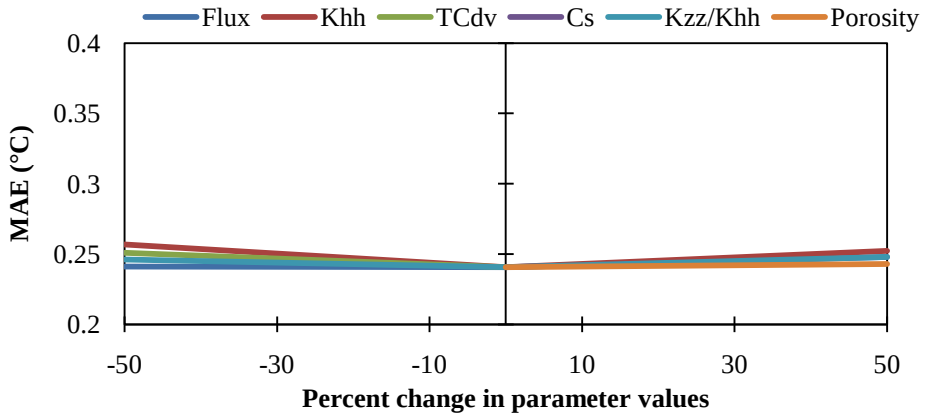

b)

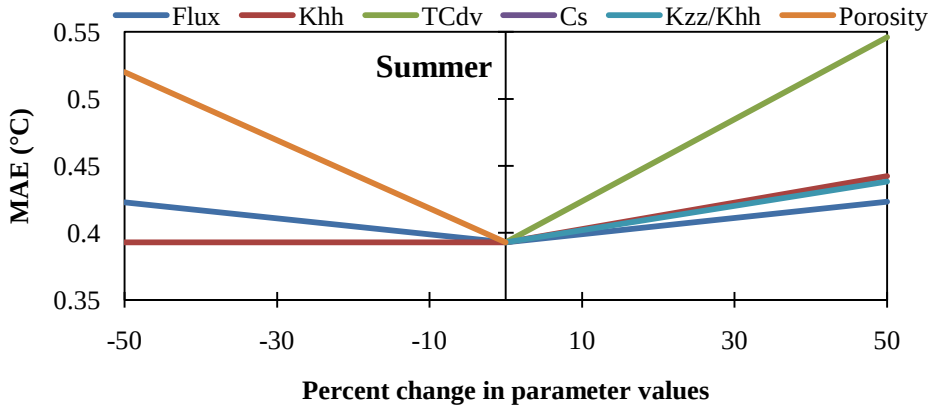

c)

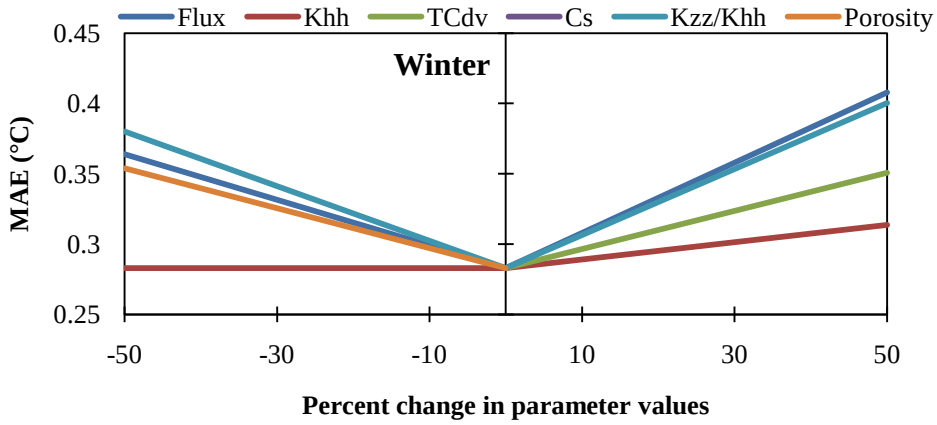

Figure 20 Model sensitivity analysis for a) Spring, b) Winter and c) Summer models.

CHAPTER V

DISCUSSION

The distribution of substrate temperature is based on stream and ground temperatures, fluctuations of stream temperatures and the nature of water flow from stream water to ground water and vice versa. The importance of stream water fluctuations on streambed was evident by the fact that temperature fluctuations in the substrate were highest for summer and spring than during the winter and were dependent on the range of temperature of stream water itself (Table 3).While some of the temperature fluctuation for the spring model period can be due to the small storm events that occurred during the time period, the higher fluctuations in streambed temperatures during the summer is a marked difference from the winter. Hence, the greater temperature range of over 0.3°C observed at 150 cm depth during the summer model period suggests a greater influence of stream water temperatures on the substrate compared to less than 0.3°C observed at 60 cm depth during the winter model period.

When looking at After-Storm Substrate Temperature Change (ASSTC), Oware (2010) found that there was significant difference in ASSTC from 30 cm depth to 150 cm depth during the winter while no significant difference between the two depths were found during the summer. The similarity in ASSTC over the various depths during the summer was attributed to the warmer summer water penetrating the streambed deeper than the cold winter water. Although, density differences and associated viscosity differences could be a major factor in the deeper penetration to stream water in the

substrate as put forward by Oware (2010), similar role of density and viscosity change may not be inferred to non storm time periods where temperature difference in the streambed from summer to winter at 60 cm depth is less than 10°C and that at 90 cm is only about 4°C. A greater role in the comparatively deeper penetration of temperature fluctuations during the summer in both storm and non-storm time periods could be attributed to the smaller upwelling during the summer that allows for deeper hyporheic flows compared to winter.

Comparison of vertical flux across the bottom boundary suggests a comparatively higher flux value for the winter model period. While stage during the winter model period is slightly higher than that during the summer model period, no relation can be established between stage and upward flux over all three models because stage was on average higher during the spring model period than that during the winter model period (Figure 7). Possible explanation could be found in the difference in evapotranspiration rates between summer and winter and in the nature in which recharge occurs from winter snow. The rate of evapotranspiration is very high during summer compared to winter and the loss of ground water from shallow aquifers to the atmosphere due to evapotranspiration can lower water table, and consequently lower the hydraulic gradient between the aquifer and the gaining stream. This could also result in relatively smaller base flow into the stream during summer as compared to winter.

Walton (1965) suggested that evapotranspiration in Illinois is so high during the summer that little precipitation percolates into the water table except during periods of excessive rainfall. Snow pack during the winter provides for a sustained source of recharge into shallow aquifers and can be expected to result in higher base flow to stream

even when there is no precipitation. Although, no soil temperatures are available in the vicinity of the study site, soil temperatures recorded in nearby Peoria, IL for the time period between Jan 15-21(winter model period) suggested that the ground went through diurnal freeze and thaw cycles at a depth of 0.1 (Water and Atmospheric, 2010). Ground freezing was absent during the model period at a depth of 0.2m which shows the moderating effect of warmer temperatures at depth on the ground surface. A detailed study on the snow melt and ground freezing patterns in the study site during the winter will be needed to better establish the role of snow pack on base flow. Since, precipitation in the region is comparatively higher during the summer months than the winter months; the importance of decreased evapotranspiration and snowpack melting during winter on increasing base flow could be higher than the vertical flux values reflect.

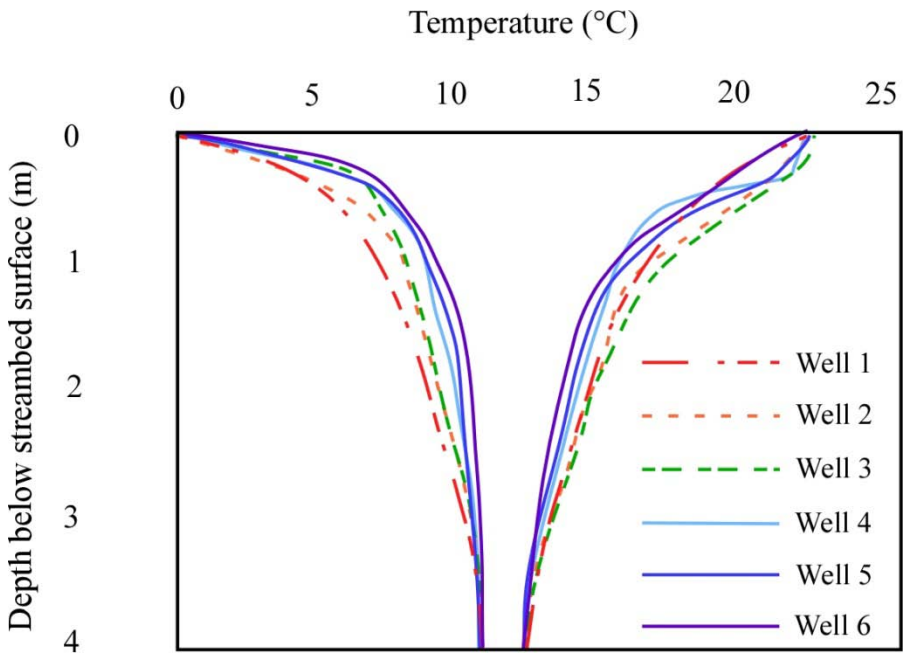

Figure 21 Temperature envelopes for Well 1-6.

Upward contracting temperature envelope for the wells in the site suggests that the stretch is upwelling with annual temperature fluctuations of less than 8°C and 3°C at depths of 150 cm and 4m respectively. In a system without advection annual temperature fluctuations of about 12°C at a depth of 150 cm and of about 4°C at a depth of 4 m is seen (Lapham, 1989). Comparison of temperature envelopes for various wells over the period of one year suggests a comparatively higher upwelling in Well 4-6 as compared to Well 1-3 (Figure 21). The difference in temperature envelopes spatially is likely topography driven because of riffle and pool sequence although spatial heterogeneity could also contribute to the trend. Relatively higher upwelling in Well 5 and 6 falls in the downstream pool where hyporheic flows were expected to rejoin the stream (Figure 11). It can thus be implied that upwelling is influenced by topography induced flow. Less upwelling is associated with areas where stream water enters the hyporheic zone and more upwelling is associated with areas where hyporheic water reenters the stream. This also highlights the importance of the upstream parts of pools in riffle and pool sequences on providing a more sustainable environment to benthic organisms, especially during the winter, where they are under the influence of stable ground water temperatures the most.

Specifically, temperature envelope on the winter side showed inflection at 30 cm depth as compared to the 90 cm depth for the summer side suggesting a greater influence of ground water temperatures on the streambed substrate than during the summer. This difference was also represented by the models (Figure 14 and Figure 15) where streambed temperature fluctuations were observed to a relatively deeper depth in the summer model compared to the winter model. The streambed is thus more stable during the winter because of the greater upwelling than during the summer. This also results in

the lower model errors for the winter model period at shallow depth compared to the summer model period.

Changes in horizontal hydraulic conductivity (Kh) between the three models were small and the model sensitivity to Kh in its range is small compared to the accuracy of the loggers, suggesting there was no discernable difference in overall Kh values between the models. While looking at the temporal variability of hydraulic conductivity (Kh) in a gaining agricultural stream, Genereux et al. (2008) suggested a significant variability that was not due to variation in temperature but as a result of deposition and erosion induced changes in the streambed. The study also suggested that lower Kh values were associated with streambed areas with higher amounts of finer sized particles and that decrease in hydraulic conductivity with depth may be expected if the streambed is homogeneous. In a study done on the 600 m stretch of LKC immediately upstream on the study site, Peterson et al (2008) suggested significant streambed mobilization during larger storm events. Such storm events result in a higher Kh streambed in the top portion of the streambed that can be expected to decrease over time when the particles realign, get compacted and pore spaces between coarse sediments are filled in by finer particles. Alongside, higher positive errors during summer and some negative errors during winter at 30 cm depth tells us that stream temperature influence is more prominent at 30 cm depth than the deeper substrate and suggests the top of the streambed has higher hydraulic conductivity than the lower part. Importantly, the layer of streambed mobilized is very shallow compared to the streambed thickness used in the model, implying that the actual changes in hydraulic conductivity of the dynamic streambed top could be significant although not represented by the models built in this study. In addition, since the model is assumed to

be homogeneous and does not well represent the higher hydraulic conductivity of the shallow substrate, the heat transfer to shallow substrate due to hyporheic flows cannot be accurately represented by the model.

Simulated temperature values were mostly comparable to the observed values (Figure 19) and are in line with error ranges in previous studies using VS2DH (Constantz et al, 2003; Conlon et al, 2003,) and other unspecified numerical models (Hoffman et al 2003; Prudic et al, 2003). It is important to note that all of these aforementioned models were used to simulate either smaller range of depth or lateral distance and this difference in set up is one of the most distinct differences for the model used in this study. The model does not simulate the temperature at 30 cm as well as it simulates the deeper streambed temperatures because model calibration is based on MAE of all the observation points. Thus, the dynamic shallow substrate with only 4 observation points is not as well represented compared to the deeper substrate with 12 observation points. Consequently the more dynamic and likely hydraulically and thermally different upper layer is not as well represented by the model.

In-stream structures are known to influence streambed temperature via induced hyporheic exchange (Hester et al, 2009). Some changes to the stream flow can be expected because water has to flow around the wells and around foreign objects caught in the well. The exact effects of these impedances on stream flow and subsequently on hyporheic flow and hyporheic temperature is unknown and will be considered uncertainity. Since, streambed topography plays an important role in induced hyporheic flow paths, large objects caught around the wells may cause deviation from expected temperature patterns in the shallow substrate. Further, the model's ability to properly

predict induced flows can be hindered if the topography along the thalweg is significantly different from the sides. Importantly, the induced hyporheic flows simulated by the model is dependent on points along the upper boundary where total head change is defined and may not accurately represent the actual location of induced hyporheic flow in the shallow substrate. This limitation may also result in deviations from observed temperatures thereby resulting in higher errors at 30 cm observation points.

A study of thermal Peclet numbers in the streambed provides valuable information of the temporal and spatial dynamics of the hyporheic zone. When an interaction of a one dimensional conductive thermal field occurs with a one dimensional advective flow field in the same plane, the distribution of conduction induced temperatures is altered and the nature of this alteration can be represented by a ratio of advective to conductive heat transfer known as thermal Peclet number (Pe):

$$\mathrm{Pe} = \frac{\rho_w c_w q l}{k_t} \tag{2}$$

where, $\rho_w c_w$ is the volumetric heat capacity of water, l is the length scale, q is the advective velocity associated with the length scale and k_t is thermal conductivity of the saturated medium. Pe, positive or negative, of 1 suggests an equal role of advective and conductive heat transfer, Pe >1 suggests dominance of advective transport over conductive transport and Pe <1 suggests that conduction is dominant mode of heat transport.

Table 5 Table of Peclet numbers for various wells during the three model periods.

Spring*					Summer‡					Winter†			
W1	W2	W3	W4	W5	W1	W2	W3	W5	W6	W1	W3	W5	W6
4	2	3	4	0.5	3	2	2	2	3.5	3.5	3.5	3.75	4

*Well 6 not installed yet.
‡ Well 4 and 6 had malfunctioning loggers at 90 cm and 150 cm respectively.
†Well 2 had malfunctioning logger at 150 cm.

Peclet numbers suggest that advection plays a more dominant role in heat transport than conduction in the streambed. Temperature curve displacement in the upward direction suggests that the direction of advection is in the upward direction in all three model time periods hinting that the stretch is perennially a gaining stretch. Consistently higher Pe for the winter model period as compared to the spring and summer time period validate the higher upward flux values obtained for the winter model. Also, the variations in the Peclet numbers either represent differences in thermal conductivity or advective rates along the stretch of the study area. Since thermal conductivity changes little between earth materials, some spatial heterogeneity may be causing variations in the vertical hydraulic fluxes.

Also, in hindsight, Pe values for these non-storm time periods were drastically smaller than the overall Pe determined by Oware (2010), i.e. 34.1, suggesting an even greater role of advection in streambed heat transport in the immediate aftermath of a storm event, and highlights the difference in streambed thermal regime associated with storm and base flow periods. Caution must thus be taken when doing numerical modeling of streambed involving storm events.

CHAPTER IV

CONCLUSION

LKC goes through temperature reversals between summer and winter with the stream at higher temperature than ground water during the summer and at lower temperature during the winter. During spring and likely during fall, the streambed has low temperature gradient with very little variation in temperature from stream water to ground water. Streambed temperatures curves contract closer to the surface during the winter than during the summer and the observation is pronounced in areas with higher upwelling like the upstream reaches of pools in a riffle and pool sequence Numerical models using VS2DH are not sufficiently sensitive to parameter changes for the spring suggesting the limitation of using the model to low temperature gradient periods to adequately discern differences .from summer and winter. Vertical flux in the upward direction is lower during the wetter summer season than during the drier winter likely due to greater evapotranspiraton during the summer and sustained percolation into the shallow aquifer from the snow during the winter. The yearlong upwelling in the study area has a stabilizing effect on most of the streambed. The effect of thermally variant stream temperature is restricted to the shallow substrate and during upwelling conditions like the one seen in the site, no overall change in other hydraulic and thermal parameters is observed.

Overall, second to temporal changes in thermal gradients, vertical flux was the most dominant parameter in imparting differing temperature profile to the streambed.

Seasonal changes in other parameters like hydraulic conductivity, porosity, vertical anisotropy and heat capacity are very small or nonexistent and determining any changes in these parameters will require controlled laboratory experiments.

REFERENCES

Alexander M.D., Caissie, D., 2003, Variability and comparison of hyporheic water temperatures and seepage fluxes in a small Atlantic salmon stream, Ground Water, v. 41, no. 1, p. 72-82.

Anderson, M.P., 2005, Heat as a ground water tracer: Ground Water, v. 43, no. 6. p. 951-968.

Bartolino, J.R., Niswonger, R.G, 1999, Numerical simulation of vertical ground-water flux of the Rio Grande from ground-water temperature profiles, central New Mexico, U.S. Geological Survey Water-Resources Investigations Report 99-4212, p. 34.

Beach, V., 2008, The impact of streambed sediment size on hyporheic temperature profiles in a low gradient third order agricultural stream, Master's Thesis for Department of Geography-Geology, Illinois State University.

Boulton, A.J., Findlay, S., Marmonier, P., Stanley, E.H., Valett, H.M., 1998 The functional significance of the hyporheic zone in streams and rivers, Annual Review of Ecology and Systematics, v. 29, 59-81.

Bravo, H. R., Jiang, F., 2002, Using groundwater temperature data to constrain parameter estimation in a groundwater flow model of a wetland system, Water Resources Research, v. 38, no. 10.1029/2000WR000172.

Brederhoeft, J.D., and S.S. Papadopulos, 1965, Rates of groundwater movement estimated from the earth's thermal profile: Water Resources Research, v. 1, no. 2, p. 325-328.

Bukata, P. R., Jerome, J. H., Kondratyev, K.Y., Pozdnyakov, D. V., 1995, Optical properties and remote sensing of inland and coastal waters, CRC, USA, P. 37.

Caissie, D., 1991, The importance of groundwater to fish habitat: Base flow characteristics for three Gulf Region rivers, Canadian Data Report of Fisheries and Aquatic Sciences, no. 814.

Cardenas, M.B., Harvey, J.W., Packman, A.I., Scott, D.T., 2008, Ground-based thermography of fluvial systems at low and high discharge reveals potential complex thermal heterogeneity driven by flow variation and bioroughness, Hydrological Processes, v. 22, p. 980-986.

Conlon, T., Lee, K., Risley, J., 2003, Heat tracing in streams in the central Willamette Basin, Oregon, In Heat as a Tool for Studying the Movement of Ground Water

Near Streams, ed. Stonestrom, D.A. and Constantz, J., USGS Circular 1260, p. 29-34.

Constantz, J., 1998, Interaction between stream temperature, streamflow, and groundwater exchanges in alpine streams: Water Resources Research, v. 34, no. 7, p. 1609-1616.

Constantz, J., Cox, M.H., Su, G.W., 2003, Comparison of heat and bromide as ground water tracers near streams, Ground Water, v. 41, no. 5, p. 647-656.

Gaffield, S.J., Potter, K.W., Wang, L. 2005, Predicting the summer temperature of small streams in southwestern Wisconsin. Journal of the American Water Resources Association, v. 41, no. 1, p. 25-36.

Genereux, D.P., Leahy, S., Mitasova, H., Kennedy, C.D., Corbett, D.R., 2008, Spatial and temporal variability, of streambed hydraulic conductivity in West Bear Creek, North Carolina, USA, Journal of Hydrology, v. 358, p. 332-353.

Hatch, C.E., Fisher, A.T., Revenaugh, J. S. Constantz, J., Ruchl, C., 2006, Quantifying surface water-groundwater interactions using time series analysis of streambed thermal records: Method development, Water Resources Research, v. 42, W10410.

Healy, R.W., Ronan, A.D., 1996, Documentation of computer program VS2DH for simulation of energy transport in variably saturated porous media - modification of the U.S. Geological Survey's computer program VS2DT: U.S. Geological Survey Water-Resources Investigations Report 96-4230, p. 36.

Harvey, J.W. and K.E. Bencala, 1993, The effect of streambed topography on surface-subsurface water exchange in mountain catchments, Water Resources Research, v. 29, p. 89-98.

Hester, E.T., Doyle, M.W., Poole, G.C., 2009, The influence of in-stream structures on summer water temperatures via induced hyporheic exchange. Limnology and Oceanography, v. 54, no. 1, p. 355–367.

Hoffman, J.P., Blasch, K.W., Ferré, T.P., 2003, Combined use of heat and soil-water content to determine stream/ground-water exchanges, Rillito Creek, Tucson, Arizona, In Heat as a Tool for Studying the Movement of Ground Water Near Streams, ed. Stonestrom, D.A. and Constantz, J., USGS Circular 1260, p. 47-55.

Lapham, W.W., 1989, Use of temperature profiles beneath streams to determine rates of vertical ground-water flow and vertical hydraulic conductivity, USGS Water-Supply Paper 2337.

Lu, X., Ren, T., Gong, Y., 2009, Experimental Investigation of Thermal Dispersion in Saturated Soils with One-Dimensional Water Flow, Soil Sci. Soc. Am. J., v. 73, no. 6, p. 1912-1920.

Masterson, J.P., Sorenson, J. R., Stone, J. R., Moran, S., B., Hougham, A., 2007, Hydrogeology and simulated groundwater flow in the Salt Pond region of southern Rhode Island, U.S. Geological Survey, Scientific Investigations Report 2006, p. 56.

NOAA, 2010, Climatological Data, Illinois, January 2010, v. 115, no 1 p. 3.

Oware, E.K., 2010, The impact of storm on thermal transport in the hyporheic zone of a low-gradient third-order sand and gravel bedded stream, Master's Thesis, Illinois State University.

Peterson, E.W., Sickbert, T.B., 2006, Stream water bypass though a meander neck, laterally extending the hyporheic zone, Hydrogeology Journal, v. 14, p. 1443-1451.

Peterson, E.W., Sickbert, T.B., Moore, S.L., 2008, High frequency streambed mobility of a low-gradient agricultural stream with implications on the hyporheic zone. Hydrological Processes, v. 22, p. 4239-4248.

Prudic, D.E., Niswonger, R.G., Wood, J.L., Henkelman, K.K., 2003, Trout Creek-estimating flow duration and seepage losses along an intermittent stream tributary to the humblodt River, Lander and Humboldt Counties, Nevada. In Heat as a Tool for Studying the Movement of Ground Water Near Streams, ed. Stonestrom, D.A. and Constantz, J., USGS Circular 1260, p. 57-71.

Schmidt, C., Jr., B.C., Bayer-Raich, M., Schirmer, M., 2007, Evaluation and field-scale application of a simple analytical method to quantify groundwater discharge using mapped streambed temperatures, Accepted Manuscript - Journal of Hydrology.

Silliman, S.E., Booth, D.F., 1993, Analysis of time-series measurements of sediment temperature for identification of gaining vs. losing portions of Juday Creek, Indiana. Journal of Hydrology, v. 146, p. 131-148.

Silliman, S.E., Ramirez, J., McCabe, R.L., 1995, Quantifying downflow through creek sediments using temperature time series: one-dimensional solution incorporating measured surface temperature, Journal of Hydroglogy, v. 167, p. 99-119.

Stallman, R.W., 1963, Computation of ground-water velocity from temperature data, USGS National Supply Paper 1544H H36-H46

Stallman, R.W. 1965. Steady one-dimensional fluid flow in a semi-infinite porous medium with sinusoidal surface temperature, Journal of Geophysical Research. v. 95, no 86, p. 8697- 8704.

Stanford, J.A., Ward, J.V., 1993, An ecosystem perspective of alluvial rivers: connectivity and the hyporheic corridor. Journal of the North American Benthological Society, v. 12, no. 1, p. 48-60.

Stonestrom, D.A., Constantz, J., 2004, Using temperature to study stream-ground water exchanges, USGS Fact Sheet 2004-3010.

Su, G.W., Jasperse, J., Seymour, D., Constantz, J., 2004, Estimation of Hydraulic Conductivity in an alluvial system using temperatures, Ground Water, v. 42, no. 6, p. 890-901.

Suzuki, S., 1960, Percolation measurements based on heat flow through soil with special reference to paddy fields, Journal of Geophysical Research, v. 65, no. 9. P, 2883-2885.

Triska, F.J., Kennedy, V.C., Avanzino, R.J., Zellweger, G.W., Bencala, K.E., 1989, Retention and transport of nutrients in a third-order stream in Northwestern California: Hyporheic Processes, Ecology, v. 70, no. 6, p. 1893-1905.

U.S.EPA, 1986, Saturated Hydraulic Conductivity, Saturated Leachate Conductivity and Intrinsic Permeability, EPA Method 9100, Cincinnati, OH.

Water and Atmospheric Resources Monitoring Program. Illinois Climate Network. (2010). Illinois State Water Survey, 2204 Griffith Drive, Champaign, IL 61820-7495.

Weight, W.D., 2008, Hydrogeology Field Manual, New York, McGraw Hill, p. 97,107, 266-7.

White, D.S., 1993, Perspectives on defining and delineating hyporheic zones. Jounal of North American Benthological Society, v. 12, no 1, p. 61-69.

Winter, T.C., Harvey, J.W., Franke, O.L., and Alley W.M., 1998, Groundwater and surface water a single resource. USGS Circular 1139, Denver.

APPENDIX A

SCOUR AND FILL AND ELEVATION DATA

		Marker 1	Marker 2	Marker 3	Marker 4
20-May-09	Current	37.2	33.7	22.2	37.9
19-Jun-09	Current	47.5	43.0	34.3	47.0
	Reset	42.8	43.0	34.3	36.8
	Scour	10.3	9.3	12.1	9.1
	Fill	4.8	0.0	0.0	10.3
9-Jul-09†	Current	42.2	41.9	34.9	43.8
	Reset	42.2	41.9	34.9	38.7
	Scour	-0.6	-1.1	0.7	7.1
	Fill	0.0	0.0	0.0	5.1
4-Sep-09	Current	44.0	42.0	38.5	47.5
	Reset	43.5	41.0	37.0	42.8
	Scour	1.8	0.1	3.6	8.8
	Fill	0.5	1.0	1.5	4.8
10-Oct-09*	Current	44.0	39.0	34.5	41.0
	Reset	40.0	38.0	32.0	41.0
	Scour	0.5	-2.0	-2.5	-1.8
	Fill	4.0	1.0	2.5	0.0

†Negative scour values are likely from errors in measurements between inch based and metric measuring sticks.

*Scour and fill markers were starting to tilt and bend and should explain negative values in scour.

ID	Distance (m)	Top Elev.(m)	Stream bed elev. (m)					
			Initial (Feb)	20-May	19-Jun	9-Jul	4-Sep	10-Oct
Well1	0.00	2.46	1.86	n/a	n/a	n/a	n/a	1.94
Well2	5.04	2.25	1.65	n/a	n/a	n/a	n/a	1.74
Marker1	7.35	2.15	n/a	1.805	1.75	1.74	1.715	1.75
Well3	10.09	2.29	1.69	1.855	1.8	1.79	1.765	1.8
Marker2	13.16	2.13	n/a	1.843	1.74	1.74	1.72	1.75
Well4	14.95	2.32	1.72	1.913	1.81	1.81	1.79	1.82
Marker3	18.28	2.17	n/a	1.97	1.9	1.87	1.82	1.85
Well5	19.75	2.23	1.63	1.87	1.8	1.77	1.72	1.75
Marker4	22.96	2.12	n/a	1.7	1.73	1.75	1.69	1.71
Well6	24.66	2.15	1.55*	1.64	1.67	1.69	1.63	1.65

*Projected streambed elevation based on changes in Well 5

APPENDIX B

TRACER TEST DATA

Time (min)	Stream Br^-	1A	1B	1C	1D†	2A	2B	2C	2D†	3A	3B	3C	3D
0	0.09	0.13	0.12	0.14	*	n/a	0.09	n/a	*	n/a	0.08	n/a	n/a
5	3.06	0.09	n/a	n/a	*	0.11	0.10	n/a	*	0.13	0.12	0.13	0.14
15	2.35	0.10	n/a	0.09	*	0.81	0.45	n/a	*	0.12	0.13	0.13	0.14
25	1.59	0.11	n/a	0.17	*	1.07	1.43	0.15	*	0.13	0.13	0.13	0.12
35	0.39	0.09	0.13	0.15	*	1.01	n/a	0.12	*	0.13	0.12	0.12	0.13
45	0.18	n/a	n/a	n/a	*	0.53	0.61	n/a	*	n/a	n/a	n/a	n/a
55	n/a	0.07	0.11	n/a	*	1.00	0.59	n/a	*	n/a	n/a	n/a	n/a
65	2.80	n/a	0.13	n/a	*	0.91	1.46	0.13	*	n/a	0.10	n/a	n/a
75	32.06	n/a	0.08	0.09	*	7.92	1.30	0.12	*	0.08	0.09	0.09	n/a
85	26.32	0.12	0.09	n/a	*	4.25	7.08	0.14	*	0.10	n/a	n/a	n/a
95	30.86	0.08	0.08	n/a	*	8.44	n/a	n/a	*	0.13	n/a	n/a	0.06
105	3.73	0.11	n/a	n/a	*	10.62	9.22	0.08	*	n/a	n/a	n/a	n/a
115	9.75	0.09	n/a	0.10	*				*	0.07	0.07	0.07	n/a
125	8.15	*	*	*	*	n/a	4.88	n/a	*	*	*	*	*
130	7.72	*	*	*	*	1.61	4.82	n/a	*	*	*	*	*
145	10.90	n/a	n/a	0.09	*	*	*	*	*	0.10	n/a	n/a	0.05
160	2.35	*	*	*	*	1.19	5.32	n/a	*	*	*	*	*
175	0.56	n/a	n/a	0.10	*	*	*	*	*	n/a	n/a	n/a	0.05
190	0.26	*	*	*	*	1.13	1.29	n/a	*	*	*	*	*
220	0.26	0.04	n/a	n/a	*	*	*	*	*	n/a	n/a	n/a	0.13
250	n/a	*	*	*	*	0.13	0.07	n/a	*	*	*	*	*
280	n/a	n/a	n/a	0.03	*	*	*	*	*	0.03	n/a	n/a	n/a
310	n/a	*	*	*	*	0.11	0.09	0.04	*	*	*	*	*
340	n/a	0.04	n/a	n/a	*	*	*	*	*	n/a	n/a	n/a	n/a
370	0.12	*	*	*	*	0.07	0.12	n/a	*	*	*	*	*
430	n/a	n/a	0.05	n/a	*	*	*	*	*	n/a	0.04	n/a	n/a
490	0.14	*	*	*	*	0.14	0.15	n/a	*	*	*	*	*
550	n/a	n/a	n/a	0.08	*	*	*	*	*	n/a	0.13	0.07	n/a
610	0.14	*	*	*	*	0.15	0.10	n/a	*	*	*	*	*
670	0.15	0.13	n/a	n/a	*	*	*	*	*	n/a	n/a	n/a	0.08
720	0.11	*	*	*	*	0.15	0.22	n/a	*	*	*	*	*
780	0.08	n/a	n/a	n/a	*	*	*	*	*	n/a	0.10	0.10	0.10
840	n/a	*	*	*	*	0.11	0.10	n/a	*	*	*	*	*
900	n/a	1.00	n/a	n/a	*	*	*	*	*	n/a	n/a	0.07	n/a
1440	0.10	0.10	n/a	n/a	*	0.12	0.12	n/a	*	n/a	0.05	n/a	n/a

Appendix B

TRACER TEST DATA

Time (min)	4A	4B	4C	4D	5A	5B	5C	5D	6A	6B	6C†	6D†	LK59‡
0	0.09	0.08	##	0.09	0.08	0.08	##	0.09	0.15	0.11	*	*	0.17
5	0.12	0.09	##	0.13	n/a	n/a	##	0.09	n/a	0.15	*	*	n/a
15	0.30	n/a	##	0.14	0.11	0.10	##	n/a	n/a	0.16	*	*	0.20
25	0.10	n/a	##	0.13	0.09	0.09	n/a	n/a	n/a	0.15	*	*	0.19
35	0.97	n/a	##	0.14	0.09	n/a	##	0.10	n/a	0.16	*	*	0.16
45	0.37	n/a	##	n/a	0.11	0.11	##	0.12	0.14	0.15	*	*	0.21
55	0.21	n/a	##	n/a	0.11	0.11	##	n/a	0.12	0.13	*	*	0.25
65	0.38	0.11	n/a	0.11	n/a	0.12	##	0.11	n/a	0.14	*	*	0.13
75	0.30	n/a	##	n/a	0.10	n/a	##	0.09	0.11	0.10	*	*	0.15
85	0.23	0.11	##	0.12	0.11	0.10	##	n/a	0.12	0.12	*	*	0.11
95	0.55	n/a	##	0.08	0.08	0.08	##	0.08	0.09	0.07	*	*	0.08
105	0.69	0.07	##	0.08	0.07	0.10	##	0.08	0.10	0.15	*	*	0.09
115	*	*	*	*	0.10	n/a	##	n/a	n/a	n/a	*	*	0.08
125	0.17	0.08	n/a	n/a	*	*	*	*	*	*	*	*	n/a
130	n/a	0.09	##	0.09	*	*	*	*	n/a	0.12	*	*	n/a
145	*	*	*	*	n/a	n/a	n/a	n/a	*	*	*	*	0.12
160	0.08	0.11	n/a	n/a	*	*	*	*	0.11	n/a	*	*	n/a
175	*	*	*	*	0.11	n/a	n/a	n/a	*	*	*	*	0.11
190	n/a	n/a	n/a	n/a	*	*	*	*	n/a	n/a	*	*	n/a
220	*	*	*	*	0.04	n/a	n/a	n/a	*	*	*	*	0.11
250	n/a	0.03	##	0.04	*	*	*	*	0.05	0.06	*	*	n/a
280	*	*	*	*	0.04	0.05	##	0.05	*	*	*	*	n/a
310	0.04	0.04	##	0.03	*	*	*	*	0.06	0.06	*	*	n/a
340	*	*	*	*	0.03	0.04	##	0.04	*	*	*	*	n/a
370	n/a	0.04	n/a	0.05	*	*	*	*	0.06	0.12	*	*	n/a
430	*	*	*	*	0.05	0.05	##	0.11	*	*	*	*	n/a
490	n/a	n/a	##	0.10	*	*	*	*	n/a	0.17	*	*	n/a
550	*	*	*	*	0.17	0.08	##	0.09	*	*	*	*	n/a
610	0.08	n/a	##	0.11	*	*	*	*	0.10	0.12	*	*	n/a
670	*	*	*	*	0.12	0.09	##	0.08	*	*	*	*	n/a
720	0.11	0.09	n/a	0.10	*	*	*	*	0.12	0.13	*	*	n/a
780	*	*	*	*	0.10	0.08	##	0.10	*	*	*	*	n/a
840	n/a	n/a	n/a	0.10	*	*	*	*	n/a	0.11	*	*	n/a
900	*	*	*	*	n/a	0.11	##	0.10	*	*	*	*	n/a
1440	0.09	0.05	##	n/a	0.11	0.10	##	0.05	0.13	0.14	*	*	n/a

†Samples could not be collected from a likely plugged sampling tube
‡LK59 samples were taken from a well in the west bank of LKC near W2.
*Samples were not collected

APPENDIX C

MATLAB PROGRAM TO GET ERROR OUTPUT FILE

```
% The program below creates an excel files of the errors for each of the observation points in the model
                                    198. Matrix transformations are done for both observed and model
                                    values because observed and model values are presented differently in
                                    the original files.Text in italics are explanations to the codes used.
 % This program calculates and saves errors for the summer model 198.
model_val=xlsread('model_values_81-200.xlsx','198');%[Reads the excel file for model values of model
                                    198.]
model_val=model_val(1:10752,8);%[Selects the column 8 that has the temperature values.]
Observed_val=xlsread('Observed_values.xls','JulAug');%[Reads the excel file for observed values.]
Observed_val=Observed_val(:,1:16);%[Excludes the column 17 that has pressure data]
Obs_val=Observed_val(2:end,:);%[Gets rid of the temperatures from time=0 from observed_val matrix.]
observed_val=Obs_val';              %[Transposes matrix Obs_val such that all the temp values from one
                                    time step is in row form.]
observed_val=reshape(observed_val,10752,1);%[Reshapes observed_val matrix into a 10752x 1 matrix.]
model_val=reshape(model_val,4,4,672); %[Reshapes model_val in a 4x4x672 matrix.Third dimension
                                    represents 672 time steps.]
for a=1:672                         %[Fixes inherent error in obsPoints.out file where 2B and 2C are
                                    switched for all 672 time steps.]
        b2=model_val(2,1,a);
        b3=model_val(3,1,a);
        model_val(2,1,a)=b3;
        model_val(3,1,a)=b2;
end
model_val=reshape(model_val,10752,1); %[model_val matrix is rehaped back into a 10752x1 matrix.]
for j=1:10752
ErrMat(j,1)=observed_val(j,1)-model_val(j,1);
if observed_val(j,1)==100 %[Non sampling loggers are assigned a temperature of 100 to keep the matrix
                                    size consistent.]
   ErrMat(j,1)=0;                   %[Assigns non sampling loggers an error value of 0. Care must be
                                    taken to not misinterpret these error values.]
end
end
ErrMata=reshape(ErrMat,4,4,672); %[Reshapes ErrMat into a 4x4x672 matrix.]
Filename='Errorfile_124'; %[Errorfile_sum_corrected_124 will be used as the file name to be created.]
%
%
%The following produces a new sheet for depth 30cm errors.
Sheetname1='Depth30';
ErrMatb=ErrMata(1,1,:);             %[Row 1=30 cm depth; Column 1= Well 2; all time steps.]
ErrMatc=ErrMata(1,2,:);             %[Row 1=30 cm depth; Column 2= Well 3; all time steps.]
ErrMatd=ErrMata(1,3,:);             %[Row 1=30 cm depth; Column 3= Well 4; all time steps.]
ErrMate=ErrMata(1,4,:);             %[Row 1=30 cm depth; Column 4= Well 5; all time steps.]
ErrMat2=reshape(ErrMatb,672,1);
ErrMat3=reshape(ErrMatc,672,1);
ErrMat4=reshape(ErrMatd,672,1);
```

```
ErrMat5=reshape(ErrMate,672,1);
ColHead={'Well2','Well3','Well4','Well5'};
[~,~,ElapTime]=xlsread('ElapsedTime.xls');
xlswrite(Filename,ElapTime,Sheetname1,'A1');%[Creates an excel file Errorfile_124.xls and adds a new
                                    sheet called Depth30 with elapsed time column.]
xlswrite(Filename,ColHead,Sheetname1,'B1');%[Adds the column headings in Errorfile_124.xls.]
xlswrite(Filename,ErrMat2,Sheetname1,'B2');%[Adds error for Well 2 in Errorfile_124.xls.]
xlswrite(Filename,ErrMat3,Sheetname1,'C2');%[Adds errors for Well 3 in Errorfile_124.xls.]
xlswrite(Filename,ErrMat4,Sheetname1,'D2');%[Adds errors for Well 4 in Errorfile_124.xls.]
xlswrite(Filename,ErrMat5,Sheetname1,'E2');%[Adds errors for Well 5 in Errorfile_124.xls.]
%
%
%The following produces a new sheet for depth 60cm errors.
Sheetname2='Depth60';
ErrMatb=ErrMata(2,1,:);          %[Row 1=60 cm depth; others same as Depth30.]
ErrMatc=ErrMata(2,2,:);
ErrMatd=ErrMata(2,3,:);
ErrMate=ErrMata(2,4,:);
ErrMat2=reshape(ErrMatb,672,1);
ErrMat3=reshape(ErrMatc,672,1);
ErrMat4=reshape(ErrMatd,672,1);
ErrMat5=reshape(ErrMate,672,1);
ColHead={'Well2','Well3','Well4','Well5'};
[~,~,ElapTime]=xlsread('ElapsedTime.xls');
xlswrite(Filename,ElapTime,Sheetname2,'A1');
xlswrite(Filename,ColHead,Sheetname2,'B1');
xlswrite(Filename,ErrMat2,Sheetname2,'B2');
xlswrite(Filename,ErrMat3,Sheetname2,'C2');
xlswrite(Filename,ErrMat4,Sheetname2,'D2');
xlswrite(Filename,ErrMat5,Sheetname2,'E2');
%
%
%The following produces a new sheet for depth 90cm errors.
Sheetname3='Depth90';
ErrMatb=ErrMata(3,1,:);          %[Row 1=90 cm depth; others same as Depth30.]
ErrMatc=ErrMata(3,2,:);
ErrMatd=ErrMata(3,3,:);
ErrMate=ErrMata(3,4,:);
ErrMat2=reshape(ErrMatb,672,1);
ErrMat3=reshape(ErrMatc,672,1);
ErrMat4=reshape(ErrMatd,672,1);
ErrMat5=reshape(ErrMate,672,1);
ColHead={'Well2','Well3','Well4','Well5'};
[~,~,ElapTime]=xlsread('ElapsedTime.xls');
xlswrite(Filename,ElapTime,Sheetname3,'A1');
xlswrite(Filename,ColHead,Sheetname3,'B1');
xlswrite(Filename,ErrMat2,Sheetname3,'B2');
xlswrite(Filename,ErrMat3,Sheetname3,'C2');
xlswrite(Filename,ErrMat4,Sheetname3,'D2');
xlswrite(Filename,ErrMat5,Sheetname3,'E2');
%
%
%The following produces a new sheet for depth 150cm errors.
Sheetname4='Depth150';
ErrMatb=ErrMata(4,1,:);          %[Row 1=150 cm depth; others same as Depth30.]
ErrMatc=ErrMata(4,2,:);
```

```
ErrMatd=ErrMata(4,3,:);
ErrMate=ErrMata(4,4,:);
ErrMat2=reshape(ErrMatb,672,1);
ErrMat3=reshape(ErrMatc,672,1);
ErrMat4=reshape(ErrMatd,672,1);
ErrMat5=reshape(ErrMate,672,1);
ColHead={'Well2','Well3','Well4','Well5'};
[~,~,ElapTime]=xlsread('ElapsedTime.xls');
xlswrite(Filename,ElapTime,Sheetname4,'A1');
xlswrite(Filename,ColHead,Sheetname4,'B1');
xlswrite(Filename,ErrMat2,Sheetname4,'B2');
xlswrite(Filename,ErrMat3,Sheetname4,'C2');
xlswrite(Filename,ErrMat4,Sheetname4,'D2');
xlswrite(Filename,ErrMat5,Sheetname4,'E2');
```

APPENDIX D

MATLAB PROGRAM TO CALCULATE MAE

```
% The program below calculates the mean absolute error for the model 198
model_val=xlsread('model_values_81-200.xlsx','198');%[Reads the excel file for model values of model
                                    198.]
model_val=model_val(1:10752,8);%[Selects the column 8 that has the temperature values.]
Observed_val=xlsread('Observed_values.xls','JulAug');%[Reads the excel file for observed values.]
Observed_val=Observed_val(:,1:16);%[Excludes the column 17 that has pressure data]
Obs_val=Observed_val(2:end,:);%[Gets rid of the temperatures from time=0 from observed_val matrix.]
observed_val=Obs_val';              %[Transposes matrix Obs_val such that all the temp values from one
                                    time step is in row form.]
observed_val=reshape(observed_val,10752,1);%[Reshapes observed_val matrix into a 10752x 1 matrix.]
model_val=reshape(model_val,4,4,672); %[Reshapes model_val in a 4x4x672 matrix.Third dimension
                                    represents 672 time steps.]
for a=1:672                         %[Fixes inherent error in obsPoints.out file where 2B and 2C are
                                    switched for all 672 time steps.]
        b2=model_val(2,1,a);
        b3=model_val(3,1,a);
        model_val(2,1,a)=b3;
        model_val(3,1,a)=b2;
end
%
%
s=0;
t=0;
u=0;
for i=1:672                         %[First degree loop goes through the time periods.]
for j=1:4                           %[Second degree loop goes through Well 1- 6 data.]
for k=1:4                           %[Third degree loop goes 30, 60, 90, 150cm depth data.]
x=model_val(k,j,i)-observed_val(k,j,i);
if observed_val(k,j,i)==100
t=t+1;                              %[Counter t is non-functional, the if-else statement is used to discard
                                    the loggers that did not collect data]
else
u=u+1;
s=s+abs(x);
end
end
end
end
MAErr_corrected_198=s/u             %[Returns the mean absolute error for model 198]
```